UNIVERSIDADE DA BEIRA INTERIOR
Ciências da Saúde

Production of electrospun nanofibers for tissue engineering and other biotechnologic applications

Tiago Ruivo Correia

Master Degree Thesis in

Biomedical Sciences

(2nd Cycle of studies)

Supervisor: Ilídio Joaquim Sobreira Correia, Ph. D.

Covilhã, June 2012

UNIVERSIDADE DA BEIRA INTERIOR
Ciências da Saúde

Produção de nanofibras para aplicação na Engenharia de Tecidos e noutras aplicações Biotecnológicas

Tiago Ruivo Correia

Dissertação para obtenção do Grau de Mestre em

Ciências Biomédicas

(2º ciclo de estudos)

Orientador: Prof.Doutor Ilídio Joaquim Sobreira Correia

Covilhã, Junho de 2012

Acknowledgments

This year was laborious and scientifically rewarding. Nevertheless, this task was carried out with the help of some people who I want to thank:

Firstly, I would like to express my deepest gratitude to my supervisor Professor Ilídio Correia for his guidance, patience and support during this Master Thesis. I also thank him for all the conditions and knowledge provided in this area.

I also would like to thank Eng. Ana Paula from the Optics department of Universidade da Beira Interior for the time spent on the acquisition of the scanning electron microscopy images.

To my work group for the fellowship and healthy atmosphere felt during all this year. So, I wish to thank them for supporting me through the hardest difficulties.

To my closest friends for all the courage and strength given. Also, I want to thank them for their patience and support.

Definitely, to my parents, who have been supporting me all these years. I deeply want to thank them for their unconditional guidance and faith.

“Try not to become a man of success but a man of value.”
Albert Einstein

Abstract

As a specialized and complex structure, bone is a tissue with the capacity to self-regenerate that play different functions in our body. However, when there is a critical bone defect the self-regenerative capacity is lost. Currently clinical treatments are based on bone grafts and other bone substitutes which possess several limitations. Hereupon, Tissue Engineering arises as a new scientific field that combines life sciences and engineering knowledges to create biological substitutes capable of restoring defects and lesions of biological tissues. In this context, a new strategy to mimic the extracellular matrix of bone and cellular microenvironment was developed in this work. Therefore, the electrospinning apparatus was used to produce poly(ε-caprolactone), polyethylene oxide-sodium alginate and poly(vinyl)pirrolidone nanofibers. Subsequently, the same procedure was used for coating the alginate aggregated microparticle scaffold. In addition, polycaprolactone electrospun nanofiber membranes were also produced in order to improve the mechanisms on phase separation area. These membranes were subjected to a coating process in order to improve specific properties, such as pore size, fibers diameter and surface interactions. The biological properties of the coated scaffolds were evaluated through *in vitro* cytotoxicity assays. The results showed that all the coated scaffolds had their biological performance improved when compared to the same scaffolds without coating. The membranes showed to be useful for the separation of biomolecules.

Keywords

Coating of scaffolds, electrospinning, electrospun nanofiber membrane, nanofibers, tissue engineering.

Resumo

Como uma estrutura especializada e complexa, o osso é um tecido com a capacidade de auto--regeneração responsável por muitas funções no nosso corpo. No entanto, quando existe um defeito ósseo critico a capacidade auto-regenerativa não é suficiente para reparar a lesão em causa. Na actualidade, os tratamentos clínicos baseiam-se em enxertos de osso e outros substitutos de osso que possuem várias limitações. Assim, a engenharia de tecidos surge como um novo campo científico que combina Ciências da vida e os conhecimentos de engenharia de forma a criar um substituto biológico capaz de resolver os defeitos e lesões nos tecidos biológicos. Neste contexto, uma nova estratégia para imitar a matriz extracelular do osso e o microambiente celular foi desenvolvida através deste trabalho. Um aparelho electrospinning foi usado para a produção de fibras de policaprolactona, de alginato de sódio, óxido de polietileno e polivinilpirrolidona. Este processo foi ainda usado para revestir *scaffolds* de agregados de micropartículas de alginato. Por outro lado, foram também desenvolvidas membranas à base de policaprolactona com o objetivo de serem usadas na purificação de diferentes biomoléculas. As membranas produzidas foram ainda submetidas a um processo de revestimento para melhorar propriedades específicas. A Caracterização biológica dos *scaffolds* revestidos foi realizada através de ensaios *in vitro*. Os resultados obtidos mostraram que todos os revestimentos efetuados nos *scaffolds* melhoraram o seu desempenho biológico, relativamente aos *scaffolds* sem revestimento. As membranas produzidas por electrospinning apresentaram boas propriedades, para serem testadas na separação de biomoléculas.

Palavras-Chave

Electrospinning, engenharia de tecidos, membranas de nanofibras, nanofibras, revestimento de *scaffolds*.

Index

List of Figures

List of tables

List of Acronyms

3D	Three-dimensional
AP	Alkaline phosphatase
BMP	Bone morphogenic protein
BSA	Bovine serum albumin
$CaCO_3$	Calcium phosphate
DMEM-F12	Dulbecco's modified eagle's medium
ECM	Extracellular matrix
EDTA	Ethylenediaminetetraacetic acid
FBS	Fetal bovine serum
FGF	Fibroblastic growth factor
FTIR	Fourier transform infrared spectroscopy
HA	Hydroxyapatite
MSCs	Mesenchymal stem cells
MTS	3-(4,5-dimethylthiazol-2-yl)-5-(3-carboxymethoxyphenyl)-2-(4-sulfophenyl)-2H-tetrazolium reagent, inner salt
nHAp	Hydroxyapatite nanoparticles
OI	Osteogenesis imperfecta
PCL	Poly(ε-caprolactone)
PDLLA	Poly-DL-lactide acid
PEG	Poly(ethylene) glycol
PEO	Poly(ethylene) oxide
PLLA	Polylactid acid
PS	Primary spongiosa
PVP	Poly(vinyl)pyrrolidone
SA	Sodium alginate
SEM	Scanning electron microscopy
SOC	Secondary ossification center
TE	Tissue engineering

Chapter I:
Introduction

1.1 Bone structure

Bone is a complex, highly organized and specialized connective tissue, that comprises cells and extracellular matrix (ECM) [1, 2]. It provides mechanical support to the skeleton which is fundamental for locomotion and protection of vital organs. Metabolically, bone serve as mineral reservoir of calcium and phosphorus [3]. Therefore, this tissue must be highly regulated in order to maintain the balance of the system [4]. Macroscopically, bone can be distinguish into compact (cortical), and trabecular (cancellous or spongy), due to its different density (Fig 1) [5].

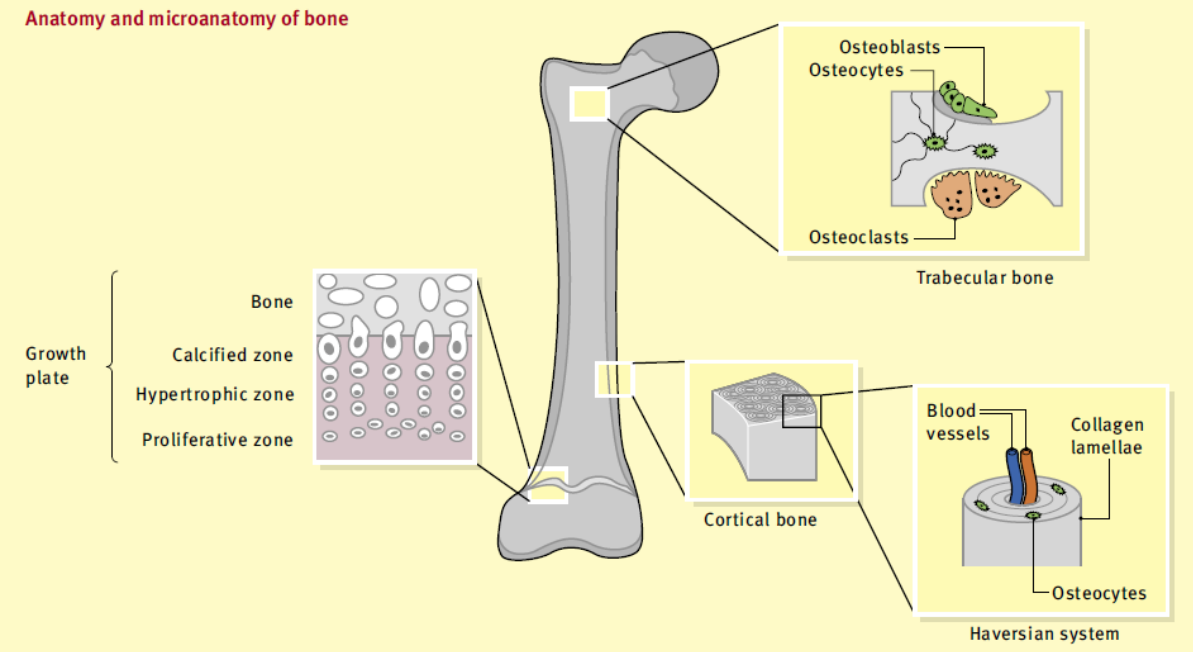

Figure 1- Representation of macroscopic and microscopic anatomy of bone (adapted from [4]).

The compact bones look like solid masses, whereas the trabecular bones are spongeous whose free spaces are filled with bone marrow. Compared to spongy bone, compact bone is denser and has on its composition osteon units that are attached one to another, but separated by interstitial and circumferential lamellae. Each structural unit contains a longitudinal central canal (Haversian canal), surrounded by 20–30 concentric lamellae of deposited collagen fibers, where osteocytes are buried within. The Haversian canal communicates to each other by Volkmann's [5]. Trabecular bone, unlike compact bone, is less dense, more porous and has a higher concentration of blood vessels. The lamellae are arranged in parallel and are mainly involved in mineral homeostasis. The pores presented in this type of bone are visible and ranging from μm to mm in size [5]. The cortical bone has an important role in tension, compression and torsion, while spongy bone mainly acts in compression. The mechanical properties of trabecular and cortical bone are listed in Table 1 [6]. Both types of bone tissue are present in specific parts of bones. Relying on shape and size, bones can be classified into

four groups: long bones, short bones, flat bones and irregular bones [5]. Trabecular bone fills the center of long bones, flat bones and vertebrae, and is an interconnecting meshwork of bony trabeculae separated by spaces filled with bone marrow [7]. Cortical bone, the majority bone, varies on its distribution. For example, it predominates in the shafts of the long bones and the femoral neck [7]. These differences are clinically significant since the trabecular bone is remodeled faster than the cortical bone, which is a consequence of its high surface area [7].

Table 1- Bone mechanical properties (adapted from [10]).

Properties	Measurements	
	Cortical bone	Trabecular bone
Young´s modulus /GPa	14-20	0.05-0.5
Tensile strength /MPa	50-150	10-20
Compressive strength /MPa	170 193	7-10
Fracture toughness /(MPa.m$^{1/2}$)	2-12	0.1
Strain to failure	1-3	5-7
Density /(g.cm^3)	18-22	0.1-1.0
Apparent density /(g.cm^3)	1.8-2.0	0.1-1.0
Surface/bone volume (mm^2.mm^3)	2.5	20
Total bone volume/mm^3	1.4x10^6	0.35x10^6
Total internal surface	3.5x10^6	7.0x10^6

1.2 Composition of bone

In order to coordinate the processes of bone formation and resorption it's fundamental that all these cellular processes are carefully regulated by the different cell types [5]. Like other connective tissue, bone is made of cells and ECM. It is composed by an inorganic phase, where hydroxyapatite (HA) comprises 70% of bone and an organic phase composed by 2% of cells and 98% of organic components from the ECM such as collagen, adhesive proteins and proteoglycans [8]. Bone comprises three types of cells, namely, osteoblasts, osteoclasts, and osteocytes (Fig.2). On bone surface, osteoblasts are responsible for the formation and organization of the ECM of bone and its subsequent mineralization as well as the synthesis of organic components. Derived from mesenchymal stem cells (MSCs), osteoblasts have the potential to be differentiated into fat cells, chondrocytes or muscle cells [9]. In addition, osteoblasts can also differentiate into bone-lining cells after bone deposition which will remain on the bone surface [2]. Osteocytes is another type of bone cells derived from osteoblasts that are responsible for intercellular communication and for breaking down the bone matrix through osteocytic osteolysis to release calcium for calcium homeostasis [10]. Osteoclasts are found at the surface of the bone and they are involved in the resorption of fully mineralized bone [11-13]. All these cells are produced through the differentiation of hematopoietic stem cells and the task of releasing acids and enzymes to dissolve the minerals and collagens present in mature bone make them highly specialized. The dissolved minerals are reused back into the blood, and their exchange on bone is controlled by the bone-lining cells, a layer of flat cells with attenuated cytoplasm and a lack of organelles beyond the perinuclear region which cover the bone surface where there is no bone growth [2].

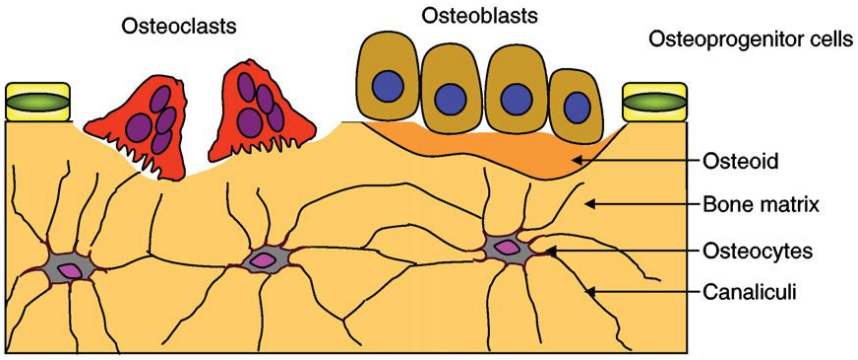

Figure 2- Schematic diagram of bone structure at a cellular level (adapted from [1]).

In bone, the ECM is composed mainly of an organic phase known as osteoid, which forms about 30% of bone mass and a mineral phase (Table 2) [8]. Relatively to the organic portion, more than 90% is composed of collagen type I and other minor collagens such as types III and V and 5% are noncollagenous proteins [14]. The noncollagenous proteins in bone include osteocalcin, osteonectin, osteopontin, adhesion proteins such as fibronectin and vitronectin, and proteoglycans such as versican, decorin, and hyaluronan [15]. The mineral phase of bone

is composed of hydroxyapatite and a calcium phosphate compound. Moreover, bone matrix, which also absorbs growth factors, acts as a reservoir of soluble inductive signals such as bone morphogenic proteins (BMPs) [8]. In bone the ECM plays a fundamental role at the structural and biological level, the mineralized matrix provides chemical cues that regulate bone cells and serves as a reservoir for ions [16]. On the other hand, collagen fibrils offer tensile strength to bone and are arranged in such a way that they form gaps between adjacent collagen molecules. These gaps are filled with hydroxyapatite crystals, that are responsible for the compressive strength of bone [16]. Furthermore, bone ECM also support bone cells through the supplying of ECM-integrin bonds that facilitate the formation of adhesive structures and active signaling pathways, that are involved in cell spreading, survival and differentiation [16].

Table 2- Composition of bone ECM [8].

			Molecular weight	Function/regulates	Binds to
Organic (30% of bone mass)	Collagens	Type I	Variable	Structural protein	Itg, TSP,OSN
		Type X	Variable	Present in hypertropic cartilage	OSP, BG, DC,BSP
		Type III	Variable	Col fibril diameter	
		Type V	Variable	Col fibril diameter	
	Adhesion proteins	Fibronectin	~400kDa	Adhesion	Itg, Col, heparin,
		Thrombospondin	~450kDa	Adhesion, bone formation	Ca, HAP, OSN
		Vtronectin	~70kDa	Adhesion	Itg, Col, heparin,
		Osteopontin	~44-75kDa	Adhesion, proliferation, resorption	Itg
		Osteonection	~35-45kDa	HAP deposition, bone formation	Ca, HAP, Col, TSP
		Osteocalcin	~5kDa	Osteoclast activity	Ca
		Bone sialoprotein	~46-75kDa	Adhesion, mineralization	Itg, Col
		Alkaline phosphatase	~80kDa	Mineralization	-
	Proteoglycans	Biglycan	~270kDa	Col fibril diameter	Col
		Decorin	~150kDa	Col fibril diameter	Col, TGF-β
Inorganic (70% of bone mass)	Hydroxyapatite	-	-	Mechanical strength of bone	-

Abbreviators used in table 2: Itg, integrins; Col, collagen; HAP, hydroxyapatite; Ca, calcium; TSP, thrombospondin; OSN, osteonectin; OSP, osteopontin; BG, biglycan; DC, decorin; BSP, bone sialoprotein; TGF-b, transforming growth factor-b.

1.3 Bone formation and repair

The skeleton formation, maintenance and reparation occurs through, two different mechanisms, the intramembranous and endochondral bone formation [17]. Intramembranous bone formation is responsible for the development of flat bones like the cranial bones and the scapula. Near the final of the second month of gestation, the formation of this type of bone starts with the condensation of loose mesenchymal tissue, that contains osteogenic cells. The beginning of ossification arises in association with adequate vascularization, and proceeds by itself. The first irregular mass of bone that is formed is known as spicule. Some of these spicules are elongated into trabeculae that by turn keep its growth and leading to the formation of trabecular bone [17]. In osteoblast regions will occur the formation of appositional bone which is characterized by the formation of osteoid layer upon layer. This step will continue until reaching the appropriate bone density. After that, bone will suffer remodelation to acquire the most optimal shape and density through simultaneous bone resorption by osteoclasts and bone formation by osteoblasts. This set of events will determine the presence of compact bone (dense) in the cortex or of cancellous bone in the interior of bones. Even with the fact that intramembranous bone formation is highly efficient, it is inappropriate for the fast longitudinal growth of the appendicular skeleton (in arms and legs) in childhood [17]. Endochondral bone formation is the mechanism responsible for the formation of long bones and lengthening (Fig.3). Typically, in this process bone is preceded by cartilage formation. In the beginning, under the influence of different fibroblastic growth factors (FGFs) and bone morphogenic proteins (BMPs), mesenchymal cells express type II collagen and differentiate into chondroblasts, that produce the cartilage matrix (anlage) [2]. A dense fibrous layer known as the perichondrium covers this anlage [17]. Primarily, a hyaline cartilage model with the common shape of the bone is produced. Once formed, the cartilage model grows by interstitial, which is responsible for the increasing of bone length and appositional growth [2]. Then, ossification centers appear in each bone, primary at center (diaphyseal) and then at the extremities (epiphysial). The enlargement and maturation of chondrocytes ends with the increasing of intracellular calcium concentration, which occurs before ossification. Serving as a substrate for calcification, the thin cartilage matrix that surrounds the hypertrophied cells coincides with death (apoptosis) of the chondrocytes. Then occurs the scaffold calcification followed by a bone deposition [17]. At the same time, the perichondrium starts to be filled with capillaries and the differentiation in periosteum takes place. The beginning of ossification is marked by the deposition of osteoid at the calcified cartilage by periosteum cappilaries and osteogenic cells. A significant part of bone is ossified except for the central canal and the two transverse plates, just beneath the epiphysis. These growth places, called physes, are responsible for bone elongation until adolescence [17].

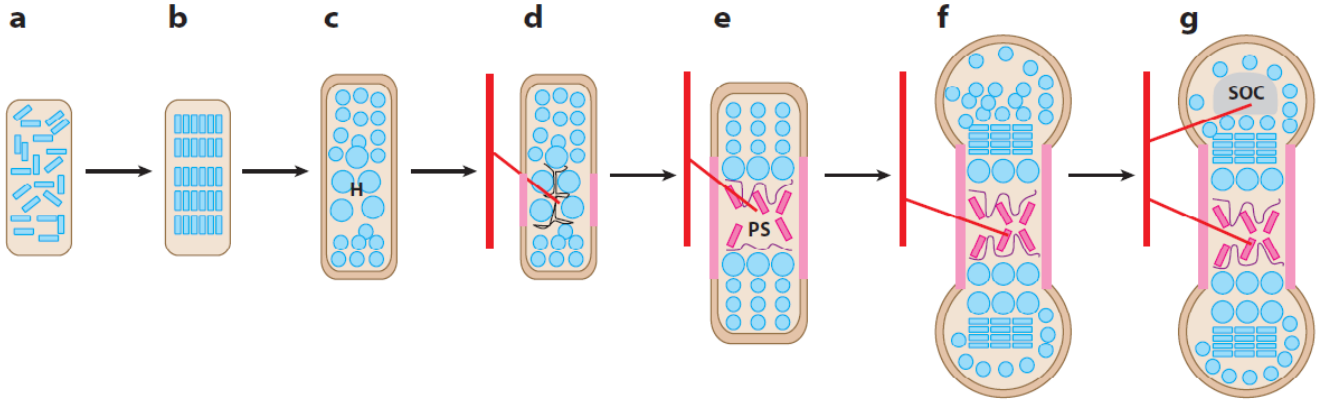

Figure 3- Schematic representation of endochondral bone formation (adapted from [18]). (a) Mesenchymal cells (blue) condense in the location of the future skeletal element. (b) Cells of condensations differentiate in chondrocytes and start to proliferate. (c) Hypertrophic chondrocyte differentiation (H). (d) Perichondrial cells differentiate in osteoblasts, forming bone collar (pink). Hypertrophic chondrocyte apoptosis favors matrix mineralization and blood vessel invasion (red). (e) Osteoblasts accompany vascular invasion, forming the primary spongiosa (PS). (f) Chondrocytes continue to proliferate, lengthening the bone. Osteoblasts of primary spongiosa form trabecular bone, while at the bone collar osteoblasts form cortical bone. (g) The secondary ossification center (SOC) forms through cycles of chondrocyte hypertrophy, vascular invasion, and osteoblast activity.

1.4 Bone disorders

Bone, like any other tissue, may be affected by several diseases, such as osteoporosis, brittle bone disease or inflammatory joints disease, among others [3]. These bone disorders can be categorized in three groups: bone inflammatory diseases, bone remodeling diseases and monogenic bone diseases [3]. Inflammatory autoimmune diseases, as a disorder of the immune system, may affect the bone integrity [19]. Normally, a systemic inflammation may result in bone mass loss through its effects on bone resorption and formation [3]. In addition, chronic inflammatory diseases (*osteomyelitis*, rheumatoid arthritis) and inflammatory diseases, (joint diseases, bowel disease, celiac disease), may lead to a reduction of bone formation and may also cause bone loss [3, 20]. In bone remodeling, the balance between bone resorption and bone formation is an essential step that guarantees the health of bone. However, factors like ageing, menopause and secondary diseases can change this physiological process and subsequently develop bone disorders in both sexes [3]. In this context, Osteoporosis arises has a skeletal disease described by a loss of bone mass and absence of biomechanical and physical assets of bone becoming susceptible to a fracture. This disorder is categorized into primary and secondary types [21]. Similarly, monogenic bone diseases can also affect the health of bone due to the abnormal production of some proteins. Moreover, an heterogeneous bone disorder of collagen, known as *osteogenesis imperfecta* (OI) or brittle bone disease, is characterized by bone fragility and decreasing of bone mass [22]. This disorder can be expressed in eight forms, specifically from type I to type VIII. The collagen type I, the most abundant protein in many tissues such as bone and skin, is reduced on the type I form of OI and it is irregular on types II, III and IV [22].

1.5 Bone grafts

As a very dynamic organ, bone regularly suffers self-remodeling and has the unique ability to repair/regenerate itself to a certain extent after an injury [5]. However, this tissue is the second most common transplanted tissue, after blood [23]. Worldwide, it's estimated that 2.2 million of bone grafting procedures are performed annually [23]. Most of the lesions that affect this tissue are caused by trauma and are relatively simple to treat; on the other hand, complex breaks and pathological fractures arising from malformation, osteoporosis, and tumors represent a difficult challenge for the treatment to be effective. In the case of elderly patients or those who suffer from severe fractures and defects, the bone´s natural healing can be seriously affected, in such a way that, mal-union or non-union of bones can only be fixed by an invasive surgery. This type of method usually uses metallic materials and requires several surgeries to repair the lesion. Subsequently the healing time is extended for a long period [24]. To overcome this problem, bone grafting has become a solution for the majority of the cases [24]. An ideal bone graft must be osteoconductive, osteogenic and osteoinductive. Osteoconductive materials allow the attachment, survival, migration, and distribution of osteogenic cells. The osteoinduction of the scaffolds provide signals that will initiate the differentiation of stem cells or progenitors towards osteoblastic cell type which will enhance bone regeneration [25]. Nowadays, the bone grafts available are grouped into three types: autogenous, allogenous and xenogenous grafts, where the first two are the most commonly used. Although these bone grafts are used for the treatment of the majority of bone defects, they still possess significant disadvantages such as limited tissue source, the hazard of adverse immunological response and pathogenic transmission [26, 27]. In this context, the new and revolutionary area called tissue engineering (TE) aims to regenerate native tissues and it represents an alternative choice to standard procedures currently used in clinical for the reparation of different kind of tissue damages. This multidisciplinary field combines principles of life sciences and engineering, with the purpose to develop biological substitutes for restoring, maintaining, or improving tissue functions [28]. Specifically, the most usual strategy for bone tissue engineering is the creation of a scaffold where osteoblasts or other cells are seeded with growth factors that stimulate cell attachment, differentiation, and the formation of mineralized bone [29].

1.6 Cell – surface interactions

The regeneration of new biological tissues is dependent on the type of the interactions between the cells and the biomaterial surface as well as its properties [30]. So, to understand those interactions, *in vitro* studies will be necessary, to the material surface. There are different factors such as underlying material, element composition and release, three-dimensional morphology, micro and nanotopography, wettability, zeta potential, and biophysical constraints under function, which may influence the cell response. Parameters as surface topography and physic-chemical surface are extremely important to understand the mechanisms of cell adhesion, to materials surface. In addition, the ions released from materials to form new bonds, can make an impact on surrounding cells [31]. However, the biological reaction determined by the topography and chemistry of the material surface is not well understood. Such fact is explained by the difficulty of testing two separate parameters from each other. This problem arises from the methods used to produce the biomaterials, which associate the two properties mentioned before. Recent studies, report that nanofiborus topography is independent of the fiber material and has revealed the capacity to modulate cell behavior such as unidirectional alignment, increased viability, attachment, and ECM production, guided migration, and controlled differentiation considered appropriate for tissue engineering [32]. As previously mentioned, the nanofibrous structure can mimic the ECM and subsequently affect cell behavior more specifically when compared to a flat culture surface. More precisely, the 3D nanofibrous structure will allow the exchange of nutrients and the utilization of receptors over the surface, while in flat conditions these interactions are limited to an exclusive side [32]. Besides these interactions, the property that had a huge impact in this context, is the high surface area to volume ratio presented by nanofibrous structures. Many authors have reported that this property increased the protein absorption, cell attachment, proliferation, differentiation and enables an improvement of cell behavior if biomolecules were incorporated in nanofibers structure [33-35].

1.7 Electrospinning

Currently, there are few methods capable of producing thin fibers such as phase separation [36], template synthesis [37], drawing [38], self-assembly [39] or electrospinning (Table 3)[40]. In the case of template synthesis the production of continuous fibers does not results. Drawing technique can only be used with viscoelastic materials. On the perspective of tissue engineering, just phase separation, self-assemble and electrospinning can be used for the production of nanofibers. However, these methods possess advantages and limitations as any other technique. Although phase separation can be used on the production of nanofibers foams, it is a time-consuming process. Similarly, self-assembly is an extremely elaborated method with low productivity of nanofibers, however it can produces thinner fibers than electrospinning technique. Hereupon, electrospinning arises as the most economical and easy method that yields continuous fibers and allow the production of nanofibers with different materials [41]. On the form of electrospun nanofibers, polymers possess some attractive attributes, such as high porosity, wide pore size range, interconnected open pore structure, a large surface area per unit volume, high flexibility, good biocompatibility and biodegradability (for fibers of biomaterials) and good modifiability [42]. Furthermore, this kind of nanofibers have exclusive mechanical properties namely tensile modulus, tensile strength; shear modulus that increases with the decreasing of fiber's diameter. Such fact can be explained by the relation between the decreasing of fiber's diameter and the increase of macromolecular chain alignment within the fibers [43]. Electrospinning is a remarkably simple technique used to produce microfibers and nanofibers from polymeric solutions or melts. Typically, the apparatus to produce the fibers requires three components: a high voltage supplier, a capillary tube with a needle of small diameter and a grounded collecting screen (Fig.4) [40].

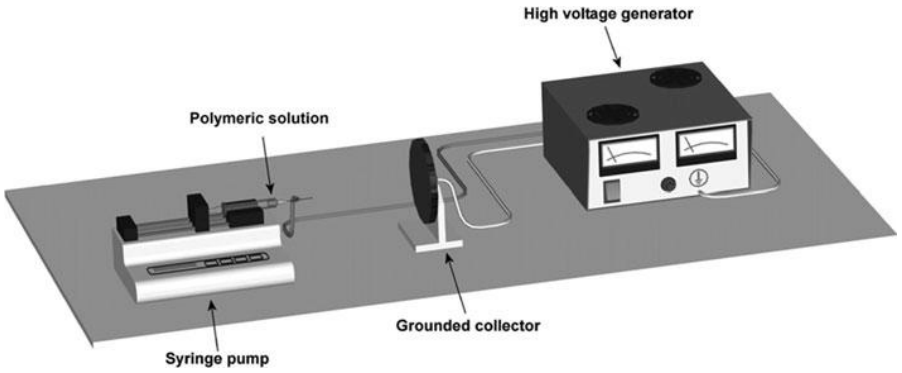

Figure 4- Schematic representation of the electrospinning apparatus (adapted from [2]).

Recently, the standard setup of this technique has been suffering an amount of modifications and updates [44-46]. Every component has an important role in the equipment. The high

voltage, from power supply, produces an electrically charged jet of polymer solution out of the needle. Then the solvent evaporates and an interconnected mesh of tiny fibers reach the collector screen [47, 48]. In this technique two electrodes are used, one is connected to the needle of spinning solution and the other is fixed to the grounded collector. The solution fluid, inside of the capillary tube, is kept by its superficial tension during the application of an electric field. This induces a charge on the surface of the liquid [44]. The mutual charge repulsion and the contraction of the surface charges to the counter electrode, origin a force directly opposite to the surface tension. With the increasing of the intensity of electrical field, the hemispherical surface of the fluid at the tip of the capillary tube also elongates, forming a conic shape named "Taylor cone" [40]. An additional increase of the electric field will generate a critical value with which the repulsive electrostatic force will overcome the surface tension of the spinning solutions and a charged jet of the fluid will be ejected from the tip of the Taylor cone. Due to the influence of electrostatic force, an instability and an elongation process is felt on the discharged polymer solution jet with the purpose of allowing it to become very long and thin. At the same time, fibers solidify as the polymer solvent evaporates, and an interlinked layer of fibers is formed on the surface of the collector [40].
The meshes, fibrous structures produced by electrospining technique, show good mechanical properties and a very high specific surface area, which are fundamental properties for their use in tissue engineering applications [49, 50]. Moreover, electrospun meshes produced with polymeric materials offer an appropriate environment for cell attachment and their production is simple and cheap [44]. Also, these meshes, due to its adjustable mechanical properties, can provide higher level of surface functionalization, protein coatings or chemical grafting of specific signaling molecules [51]. Using solo or combining fibers with other biomaterials or biomolecules allows an improvement of cells hostage [44]. One of the advantages related to the use of electrospinning technique is the capability to adjust and control the size of the produced fibers, since nanofibers closely mimic the structure of fibrous proteins, such as collagen, found in the natural ECM. This property is essential, as it has been proven before that electrospun constructs topography has an important function in cell attachment and proliferation [52, 53]. Furthermore, nanofibrous non-woven meshes are ideal for cell adhesion since a greater part of the surface is available for cell interaction [29, 54]. Moreover, the porosity of these biomaterials simplifies the nutrient transport as well as cell adhesion and the material biodegradation [28].

Table 3– Comparison of polymeric nanofiber production methods (adapted from [32]).

Method	Advantages	Disadvantages
Electrospinning	Easy to setup	Poor cell infiltration into the core of the scaffolds
	Cost effective	2-Dimensional pore or microstructure arrangement
	High level of versatility, allows control over fiber diameter, size and orientation	Toxic solvents often used
	Wide selection of materials	
Self-assembly	Easy incorporation of cells during fiber formation	Complex procedure
	3-Dimensional pore arrangement	Lack of control of fiber orientation and arrangement
	Injectable for in vivo assembly	Limited fiber diameter ~2-30nm and length ~10μm
Phase separation	3-Dimensional pore arrangement	Complex procedures
		Lack of control of fiber arrangement
Bacterial cellulose	Low cost	Limited material selection
	High productivity	Lack of versatility for functionalization
Templating	Wide selection of materials	Waste of materials
	Control over fiber diameter and length	Limitation on fiber dimensions and Arrangement
Drawing	Wide selection of materials	Low productivity (One single fiber at The time)
	Simple procedure	Difficult to form fibers with consistent diameter
Extraction	Natural materials	Limited material selection
		Limited control of fiber diameter and length (a few microns)
Vapor-phase polymerization	Polymer synthesized directly into nanofibers	Limited control of fiber diameter and length (hundreds of microns)
		Limited material selection
		Complicated procedures
Kinetically controlled solution synthesis	Polymer synthesized directly into nanofibers	Limited control of fiber diameter and length (60μm)
		Limited material selection
		Complicated procedures
Chemical polymerization of aniline	Polymer synthesized directly into nanofibers	Limited control of fiber diameter and length
		Limited material selection
		Complicated procedures

1.7.1 Parameters that influence electrospinning technique

The electrospinning process is affected by many parameters, like solution properties, processing and ambient conditions, which will subsequently influence nanofibers production [40]. Solution properties include volatility, polymer concentration and molecular weight, solvent polarity, solution conductivity, pH and viscosity. For example, if molecular weight of the polymer isn´t enough to produce a viscous solution it will not produce fibers. Other variables that must be taken in account are the processing parameters, like the applied voltage, feed rate of polymeric solution, distance between the tip and the collector, the type of collector, (if it is static or with rotation), needle diameter and the type if it is simple or coaxial, and the configuration of the nozzle. Finally, the environmental conditions such as temperature, humidity, pressure, and type of atmosphere may also influence the nanofibers production process [44, 55, 56]. There are polymers such as sodium alginate that can be influenced by the level of humidity, in such a way that if it is too high, no nanofibers will be produced. Furthermore, the solution viscosity, controlled by the amount of polymer concentration, is one of the principal determinants of nanofiber diameter and morphology. On the other hand, the increase of polymer concentration will increase the viscosity of solution which will promote uniform fibers and a decrease on fibers artefacts like beads and droplets [40]. In some cases, the liquid jet breaks up into droplets as a result of surface tension of low viscosity liquids. For high viscosity liquids the jet does not break up, but travels as a jet to the grounded target [57]. However, when solutions get too much concentrated the droplets formed at the tip of needle dry and due to that no nanofiber is produced. Thus, efforts have been made to quantify the amount of polymer concentration and viscosity to produce electrospun fibers. With the increase of solution concentration, the diameter of fibers obtained by electrospinning increased as well [40]. The solution conductivity and the charged ions in the polymer solution are highly active in jet formation. When the electric field is applied, the tension gets higher and the ions increase the charge carrying capacity of the jet [38]. The production of uniform fibers with fewer beads has been reported by the increasing of the solution conductivity or charge density [40]. Furthermore, the addition of salt, increase the solution conductivity and subsequently allows the production of uniform fibers with fewer beads. Through the addition of cationic surfactants, fibers with smaller diameters can also be obtained. Zuo *et al*. have investigated the influence of surface tension on the morphology and size of electrospun nanofibers [58]. Through the use of different solutions with various surface tensions it was found that the bead formation was affected by surface tension. Polymer molecular weight is another parameter that affects the morphology of the nanofibers, in such a way that when the concentration of polymer increases the number of beads and droplets decrease [40]. An important role in the formation of nanostructures is played by the solvent volatility which induces a phase separation process [40]. One of the most studied parameters, among other variables, is the applied voltage. Basically, in the presence of a low voltage a drop will be generated at the tip of the needle

and from that a Taylor cone will be originated from the jet. On the other hand, when the voltage is increased there are less drops causing the Taylor cone to narrow down. With the voltage increasing a larger amount of beads can be observed [48]. Other important variable is the flow rate. When the flow rate is too low, fibers with smaller diameters are produced. Otherwise, if the flow is high, fibers with beads may be presented due to a lack of time to dry before reaching the collector [40]. Besides the different parameters previously described, other factors can also influence the electrospinning process. A crucial factor in this process is the solvent used to produce the polymeric solutions. The choice of solvent is based mainly on the polymer solubility. However it is not totally correct to affirm that a higher solubility is directly related with a higher conductivity of the fluid itself [59]. A suitable solvent for electrospinning has the capability to dissolve the polymer and possesses, at the same time, a high dielectric constant (Table 4). This allows the carry of a relatively bigger amount of charges, enhancing the continuous stretching of the jet, resulting in smaller diameter fibers without beads [60, 61].

Table 4- Dielectric constants of the most used solvents in electrospinnig solutions (adapted from [56]).

Solvent	Dielectric constant
2-propanol	18.3
Acetic acid	6.15
Acetone	20.7
Acetonitrile	35.92-37.06
Chloroform	4.8
Dichloromethane	8.93
Dimethylformamide	36.71
Ethyl acetate	6.0
Ethanol	24.55
m-Cresol	11.8
Methanol	32.6
Pyridine	12.3
Tetrahydrofuran	7.47
Toluene	2.438
Trifluoroethanol	27.0
Water	80.2

1.7.2 Polymeric nanofibers

Polymeric nanofibers have a brood field of biological and medical applications (Fig.5). They possess an attractive character for areas like regenerative medicine and tissue engineering due to their ability to mimic the ECM. Acting as scaffolds, they can direct the cellular behavior and function, until the host cells are ready to repopulate and resynthesize a new natural matrix [62]. As it was previously described, the ECM of human tissue have components with nanoscale dimension. Previous studies have revealed that scaffolds with nanoscale structures support cell adhesion and proliferation, with a better performance equivalents [63, 64]. Another property that must be taken in account is the elasticity of the biomaterials that are chosen for act as a scaffold. This property, allows an elastic substrate to expand to different magnitudes similar to what happens with the different human tissues (Fig.6) [65]. The synthetic polymers like poly-ε(caprolactone) (PCL), poly(ethylene) oxide (PEO), poly(vinyl) pyrrolidone (PVP), Poly(2-hydroxyethyl methacrylate) (pHEMA) [66] have been produced for tissue engineering. Studies with these polymers have shown a favorable biological response, such as cell attachment and *in vitro* proliferation. On the other hand, in the case of natural polymers, such as sodium alginate (SA) [67], chitosan, dextran, collagen, the biocompatibility and the reabsorption of biodegradation products have increased the interest around these polymers [68]. The advantages of natural polymers include hydrophilicity, non-toxicity, lower-immunogenic reaction, cell adhesion and proliferation [69]. In this study, we report the production of electrospun nanofibers based on synthetic polymeric solutions and on the combination of natural and synthetic polymeric solutions. Also, in our group, it has been developed a non-woven mesh created by electrospinning which was used to cover the surface of the 3D scaffold. This process, so far, have only been study by few researchers [70, 71]

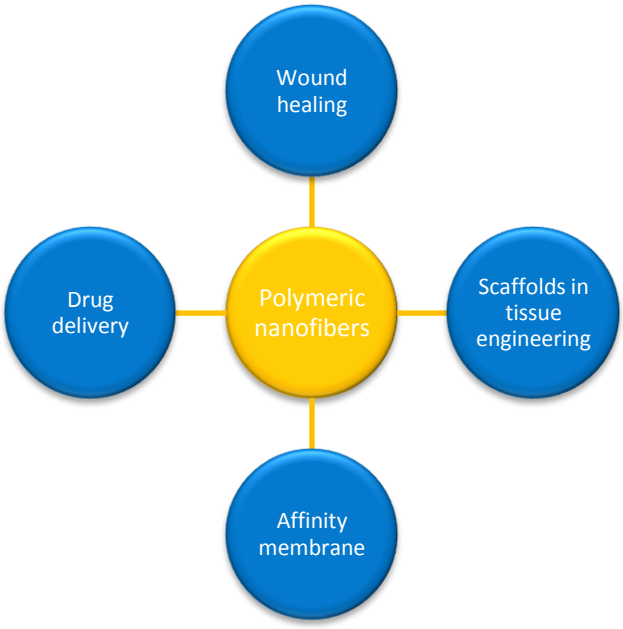

Figure 5- Polymeric nanofibers applications (adapted from [44]).

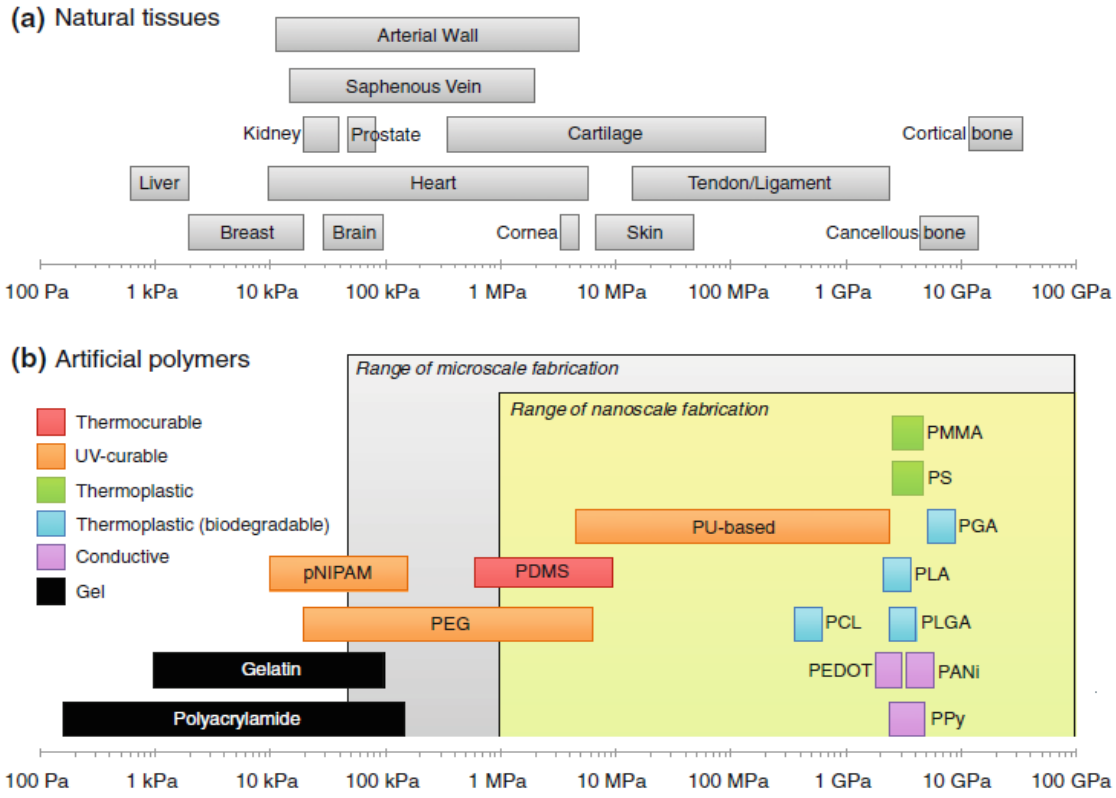

Figure 6- Scheme of mechanical properties of natural tissues and synthetic polymers. (a) Elastic modulus of different tissues in human body [65]. (b) Various biocompatible polymers used in vitro studies (adapted from [72]

1.7.3 Nanofibers applications for bone tissue engineering

The potential of nanofibers have been reported by many authors on bone tissue regeneration [73-76]. Tuzlakoglu *et al*. have studied the application of starch/PCL-based scaffolds for bone tissue engineering [74]. Through the combination of nano and microfibers and using them as a three-dimensional scaffold, they conclude that this cell carrier is capable of enhancing cell attachment, organization and a higher alkaline phosphatase (AP) activity. Yoshimoto *et al*. have also seeded PCL nanofibers scaffolds in the presence of rat mesenchymal stem cells (MSCs) [75]. They verified that, after 4 weeks of culture, cells covered the surfaces of the support matrices in multilayers. Mineralization and type I collagen were also observed in the same period. Li *et al*. explored multifunctional bioactive silk fibroin fiber-based scaffolds [73]. They have tested the scaffolds combined with bone morphogenic protein 2 (BMP-2), combined with hydroxyapatite nanoparticles (nHAp), and with both. After 31 days of seeding of human bone marrow-derived MSCs, in the presence of silk fibroin scaffolds they observed that it supported MSC growth and differentiation. Also, the combination between the silk fibroin scaffolds, BMP-2 and nHAp were associated with the highest calcium deposition and upregulation of BMP-2 increasing their potential for bone tissue engineering application. Fujihara *et al*. developed two styles of PCL nanofiber Calcium carbonate ($CaCO_{3)}$ nanoparticle composite membranes with different ratios of PCL and $CaCO_3$, 75:25 or 25:75. They verified that the osteoblasts seeded in the presence of the scaffolds showed good cell attachment and proliferation and no differences between the two membranes were found. Badami *et al*. investigated specific rat cell line alterations when submitted to different scaffolds (spin-coated glass, electrospun nanofibers of copolymers poly-DL-lactide acid (PDLLA) and polylactic acid (PLLA), block polymers PEG-PDLLA and PEG-PLLA) for study the effect of various scaffold chemical and topographical features on cell adhesion, morphology, orientation, proliferation, and osteoblastic differentiation [77]. During the 14 days of cell culture they verified an increasing on cell proliferation. Finally, they conclude that in the absence of osteogenic factors, cell density was lower on fibers than on the smooth surfaces. Controversy, in the presence of osteogenic factors cell density was equal or more than that on smooth surfaces. They also observed that cell density increased directly with fiber diameter.

1.8 Objectives

In the present study an electrospinning technique was used in order to produce coatings, with different types of electrospun nanofibers, to improve the surface area of 3D scaffold and consequently enhance of cell adhesion. Furthermore, the nanofibers produced were also assayed for biotechnological applications. The present work plan had the following aims:

- Optimization of the electrospinning process for the different polymer solutions;
- Electrospun of PCL, PEO-SA and PVP nanofibers;
- Coating 3D scaffolds with these nanofibers;
- Evaluation and characterization of the biological properties of the systems produced;
- Production of electrospun nanofiber membranes for phase separation.

Chapter II: ***Materials and Methods***

2.1 Materials

Polyethylene oxide (M_w=300,000 g/mol), polyacrylic acid (M_w=450,000 g/mol), poly(vynil pyrrolidone) (M_w=1,300,000 g/mol), sodium alginate, polycaprolactone (M_w=80,000 g/mol), acetone, phosphate-buffered saline, bovine serum albumin (BSA), dulbecco's modified eagle's medium (DMEM-F12), ethylenediaminetetraacetic acid (EDTA), L-glutamine, penicillin G, streptomycin, Amphotericin B and trypsin were purchased from Sigma-Aldrich (Sintra, Portugal). 3-(4,5-dimethylthiazol-2-yl)-5-(3-carboxymethoxyphenyl)-2-(4-sulfophenyl)-2H-tetrazolium reagent, inner salt (MTS) and electron coupling reagent (phenazine methosulfate; PMS) were purchased from Promega. Fetal bovine serum (FBS) was purchased from Biochrom AG (Berlin, Germany). Human osteoblast cells (CRL-11372) were purchased from American Type Culture Collection (VA, USA).

2.2 Methods

2.2.1 Electrospinning setup

The system herein used to carry out the electrospinning process was composed by a high power voltage supply (Spellman CZE1000R, 0–30 kV), a syringe pump (KDS-100), a syringe fitted with a stainless steel blunt end needle and an aluminum plate connected to a conductive collector (10cmx12cm). The needle was positively charged by the power supply and the metal collector was grounded. The charged tip and grounded collector form a static electric field between them, to provide the driving force that enables fiber formation [44, 78].

2.2.2 Preparation of the polymer solutions

PCL was dissolved in acetone under vigorous magnetic stirring, at a concentration of 10% (w/v). To facilitate PCL dissolution, the solution was heated at 50 ºC for a while and was sonicated for 15 minutes. [79]. PVP was dissolved in ethanol under vigorous magnetic stirring, at a concentration of 12% (w/v). The solution was sonicated for 15 minutes [80]. PEO was dissolved in water under vigorous magnetic stirring, at a concentration of 9% (w/v). At the same time SA was also dissolved in water under vigorous magnetic stirring, at a concentration of 2% (w/v). Then both solutions were mixed. The final solution was sonicated for 15 minutes [81].

2.2.3 Electrospinning setting

The solutions previously prepared were placed in a plastic syringe (10 mL), and connected through a metal syringe needle (diameter of 0.9 mm for SA-PEO and PVP solutions and a diameter of 0.8 mm for PCL solution) on the pump. The parameters of electrospinning applied were: for SA-PEO solution the flow rate was 0.6 ml/h and, the electric voltage applied was 15 kV, for PCL solution the flow rate was 3.0 ml/h and, the electric voltage applied was 18 kV and a distance between ground collector and the tip of the syringe needle of 10 cm; for PVP solution the flow rate was 1 ml/h, the electric voltage applied was 18 kV [82].

2.2.4 Scanning electron microscopy

The electrospun fibers morphology's was analyzed by scanning electron microscopy (SEM). Samples were air-dried overnight and then mounted on an aluminium board using a double-side adhesive tape and covered with gold using an Emitech K550 (London, England) sputter coater. The samples were then analyzed using a Hitachi S-2700 (Tokyo, Japan) scanning electron microscope operated at an accelerating voltage of 20 kV and at different amplifications [83]. Following, the diameter of the electrospun fibers was determined.

2.2.5 Fourier Transform Infrared Spectroscopy

In infrared spectroscopy the radiation crosses the sample and some of the radiation is absorbed, while other is transmitted. The resulting spectra represent the frequency of vibration between the atoms linkage from the sample, creating therefore, a specific spectra for those interactions [84]. The produced ENMs were analyzed and recorded on a Fourier transform infrared spectrophotometer Nicoletis 20 (64 scans, at a range of 4000 to 400cm−1) from Thermo Scientific (Waltham, MA, USA) equipped with a Smart iTR auxiliary module.

2.2.6 Nanofibers coating of alginate microparticle aggregated scaffolds

The 3D microparticle scaffolds produced by our group were coated with PCL, SA-PEO and PVP nanofibers produced by a conventional electrospinning process. The alginate microparticle aggregated scaffolds were placed between the needle tip and aluminium collector at a distance of 10 cm of the needle tip. All the solutions previously prepared (PCL, SA-PEO and PVP solutions) were placed in 10 ml syringe fitted with a certain diameter needle and the electrospinning process was carried with same parameters already tested before. To end the coating step, the alginate microparticle aggregated scaffolds were subject to electrospinning process for 15 min. In the case of PEO-SA and PVP solutions, it was necessary to expose them to a crosslinking process. For PEO-SA the crosslinking was performed by submerging the coated scaffold in a calcium chloride solution with 5% (w/v) for 12 h [67].The crosslinking process for PVP solution done at a wavelength of 254 nm [85]. All the experiments were carried out at room temperature.

2.2.7 Proliferation of human osteoblast cells in the presence of the alginate microparticle aggregated scaffolds

Human osteoblast cells were seeded in T-flasks of 25 cm^3 with 6 ml of DMEM-F12 supplemented with heat-inactivated FBS (10% v/v) and 1% antibiotic/antimycotic solution. After the cells reached confluence, they were subcultivated by a 3-5 min incubation in 0.18% trypsin (1:250) and 5mM EDTA. Then cells were centrifuged, resuspended in culture medium and then seeded in T-flasks of 75 cm^3. Hereafter, cells were kept in culture at 37°C in a 5% CO2 humidified atmosphere inside an incubator [86, 87].

To evaluate cell behavior in the presence of the scaffolds herein produced, human osteoblast cells were seeded with materials in 96-well plates at a density of $10x10^3$ cells per well, for 48 h. Previously to cell seeding, the plates and the materials were sterilized by UV irradiated for 30 min [87]. Cell growth was monitored using an Olympus CX41 inverted light microscope (Tokyo, Japan) equipped with an Olympus SP-500 UZ digital camera.

2.2.8 Characterization of the cytotoxicity profile of the alginate microparticle aggregated scaffolds

To evaluate the cytotoxicity of the scaffolds, human osteoblast cells were seeded, at a density of $10x10^3$ cells per well, in a 96-well plate, with 100 µl of DMEM-F12 and were incubated at 37°C, in a 5% CO_2 humidified atmosphere. The plates with materials were UV irradiated for 30 min, before cell seeding. After an incubation of 24 and 48 h, the mitochondrial redox activity of the viable cells was assessed through the reduction of the MTS into a water-soluble formazan product. Briefly, the medium of each well was removed and

replaced with a mixture of 100μL of fresh culture medium and 20μL of MTS/PMS reagent solution. Then, cells were incubated for 4 h at 37°C, under a 5% CO2 humidified atmosphere. The absorbance was measured at 492 nm using a microplate reader (Sanofi, Diagnostics Pauster). Wells containing cells in the culture medium without the scaffolds were used as negative controls (K^-). EtOH (96%) was added to wells that contained cells, as a positive control (K^+) [87, 88].

Cell viability results were compared with controls, in the presence of alginate microparticle aggregated scaffolds.

2.2.9 Statistical Analysis

Statistical analysis of cell viability results was performed using one-way analysis of variance (ANOVA) with the Dunnet's post hoc test. A value of $p<0.05$ was considered statistically significant.

2.2.10 Production and coating of electrospun nanofiber membranes (ENMs)

The production of electrospun nanofiber membranes was carried out using PCL solution by electrospinning process with the parameters described before. The electrospinning process was performed for 40 min in order to enable the random deposition of a large amount of nanofibers. The covering of PCL ENMs was performed using SA-PEO and PVP solutions on the conditions that were set previously. The coating was accomplished for 20 min changing the ENM position every 5 min. After, the membrane was dried at room temperature for 6 h and then crosslinked for 48 h.

Chapter III:
Results and Discussion

In this study an electrospinning apparatus was mounted and different assays conditions were tested in order to cover the surface of alginate microparticle aggregated scaffolds with different polymers (Table 5). The coatings of scaffolds were produced in order to increase cell adhesion. Furthermore, these polymers were also used to produce an electrospun nanofiber membrane, to be applied for biomolecules microfiltration process (Table 6).

3.1 Coating of the alginate microparticle aggregated scaffolds with different polymeric nanofibers

As already described before, the combination between different types of scaffold has the ability of increasing several properties such as pore size and surface area, which are considered highly important for tissue engineering. Hereupon, different polymers were used in order to compare and evaluate not only its properties such as morphology and topography, but also their cytotoxic profile. The following figure shows the scaffold used in the experimental task before and after being coated.

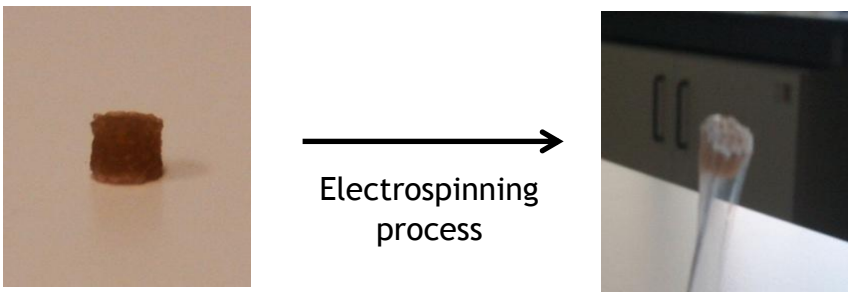

Figure 7- Macroscopic modifications of the microparticle scaffold after coating.

Macroscopically, it is possible to observe that the surface of the alginate microparticle scaffold was covered by a coating that has a similar structure to a web. In order to assure that the web formed had nanofibers, scanning electron microscopy analysis was performed.

3.1.1 Characterization of scaffolds coated with PCL nanofibers by SEM

As previously described the nanofibers have the ability to improve surface area and pore size under specific conditions. However, the optimization of the electrospinning remains a crucial step to allow the production of fibers. For this purpose, a PCL polymer with a specific molecular weight (≈80000g/mol) was used to produce nanofibers without any kind of beads (Fig.8) [89]. The nanofibers present a different range size as it can be seen in figure 13.

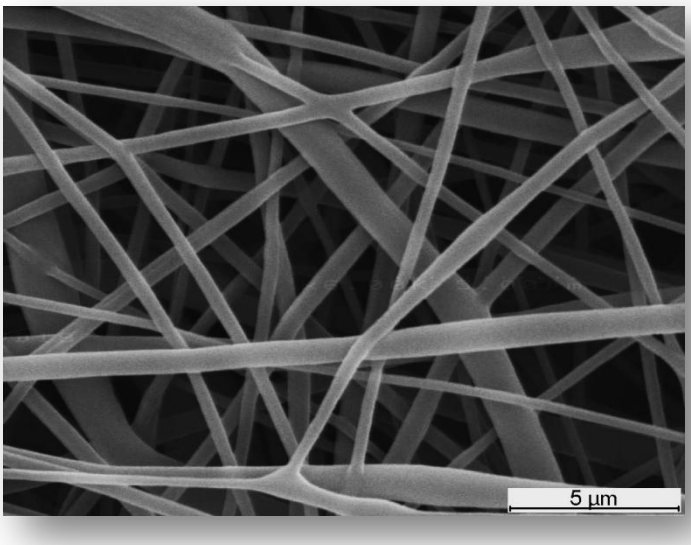

Figure 8- SEM image of the PCL electrospun nanofibers produced herein.

After the optimization of electrospinning process, the scaffold was placed on the collector to be coated with different polymers. Hereupon, the electrospinning procedure was performed under optimized conditions for a specific period of time. It was possible to observe that the surface of the scaffold was covered randomly with PCL nanofibers (Fig. 9). Through the SEM images it is possible to verify that fibers covered the surfaces of particles and the gaps between them.

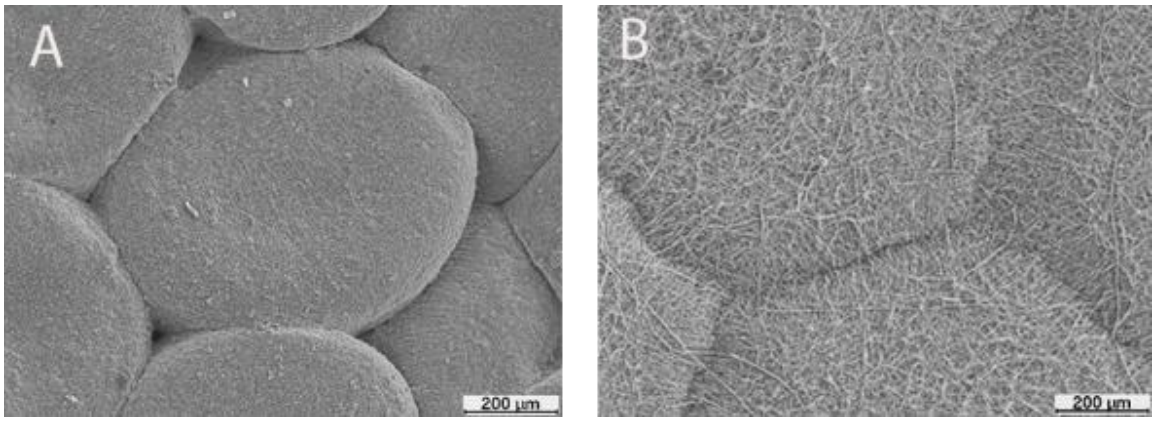

Figure 9- SEM images of microparticle aggregated scaffold before (A) and after (B) being coated with PCL.

3.1.2 Characterization of scaffolds coated with PEO-SA nanofibers by SEM

Another solution, formed by a mixture of PEO and SA, was used in order to modify some properties of scaffolds such as fibers diameter and pore size dimension. The electrospinning apparatus was also optimized to decrease the defects of fibers such as beads and droplets (Fig.10). The nanofibers above show a thinner diameter, absence of beads between them and a random orientation (Fig.13). The thinner diameter of fiber is due to the low flux applied during the electrospinning process.

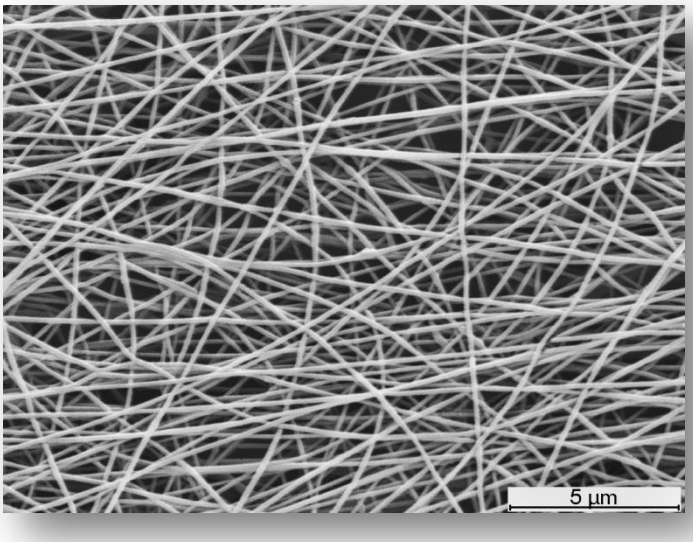

Figure 10- SEM image of PEO-SA electrospun nanofibers.

It is known that a single polymer cannot satisfy all the requirements of an ideal biomaterial [90]. Therefore, other combination of polymers, PEO and SA, was used with the purpose to evaluate the density of fibers on the mesh produced. Similarly, the electrospinning process was also used to coat another microparticle aggregated scaffold (Fig.11). The coating was made with thinner nanofibers with different morphology from those made with PCL.

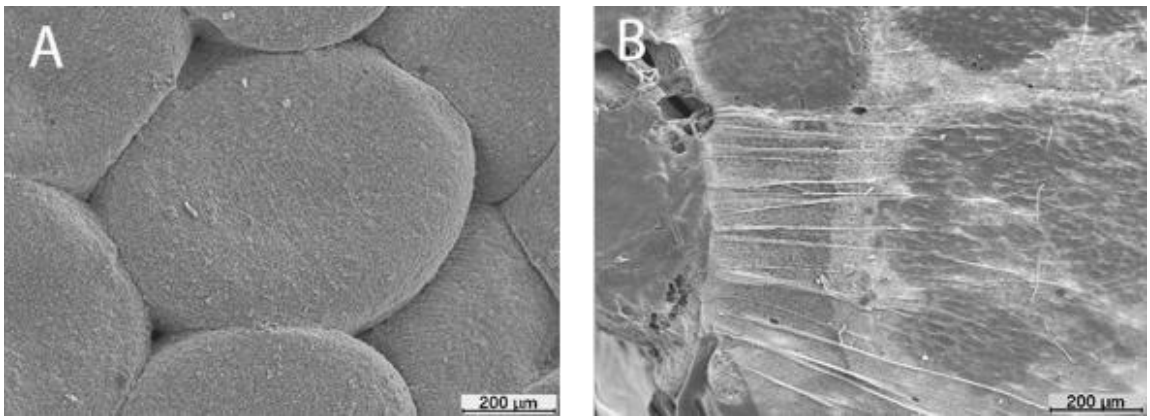

Figure 11- SEM images of microparticle aggregated scaffold before (A) and after (B) being coated with PEO-SA.

3.1.3 Characterization of scaffolds coated with PVP nanofibers

Nanofibers of PVP polymer were also produced (Fig.12). The objective of this part of the study was to evaluate the mechanical differences, such as pore size and fibers diameter, when using an hydrophilic polymer. The nanofibers apparently have a similar aspect those previously produced in our study, however these ones have a diameter around 600-700nm (Fig.13). They also present a random distribution that form interconnected voids.

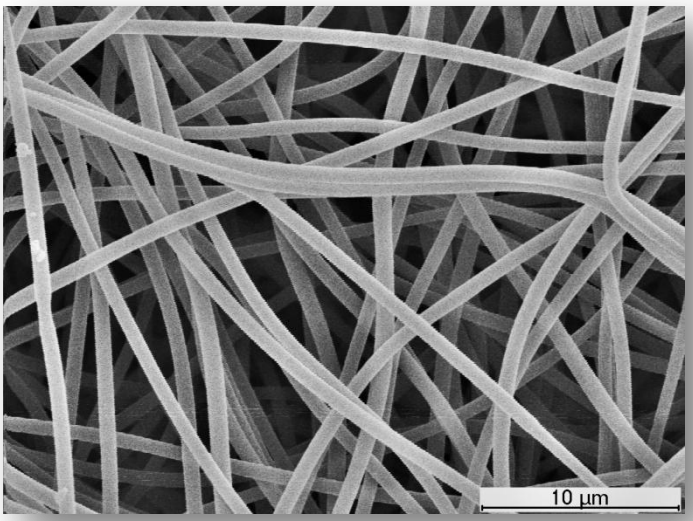

Figure 12- SEM image of PVP electrospun nanofibers

The size that they present can be explained by the high voltage applied during electrospinning process. The nanofibers presented an uniform size (see figure 13).

Table 5- Parameters of electrospinning.

Polymer solution	Solvent	Concentration (%)	Coating time (min)	Fibers size (nm)	Flux (mL/h)
PCL	Acetone	10	10	236 - 1114	3
PVP	Ethanol	12	10	725 - 806	1
PEO-SA	Distillated water	9-2	10	119 - 171	0,6

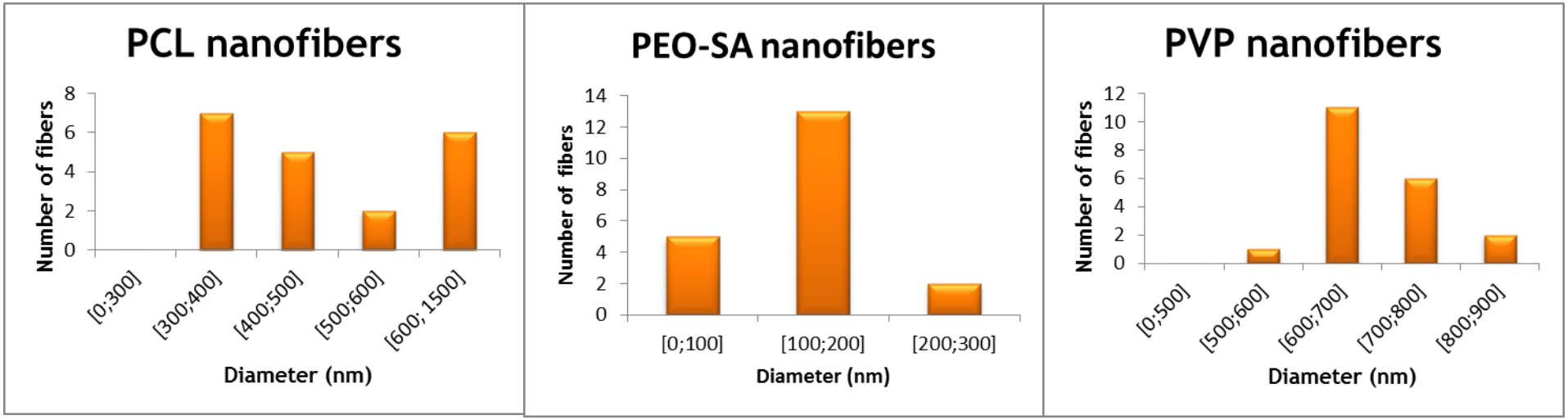

Figure 13- Comparison of the size of different polymeric nanofibers.

3.2 Characterization of electrospun nanofiber membranes (ENMs)

The electrospun nanofiber membranes were produced in a similar way using the electrospinning apparatus. A non-woven mesh was produced by the accumulation of fibers in the collector. Macroscopically, it was possible to observe a homogenous membrane (Fig. 14 A). On the other hand, SEM images show the mesh that is composed by nanofibers with several diameters and with random orientation (Fig.14 B).

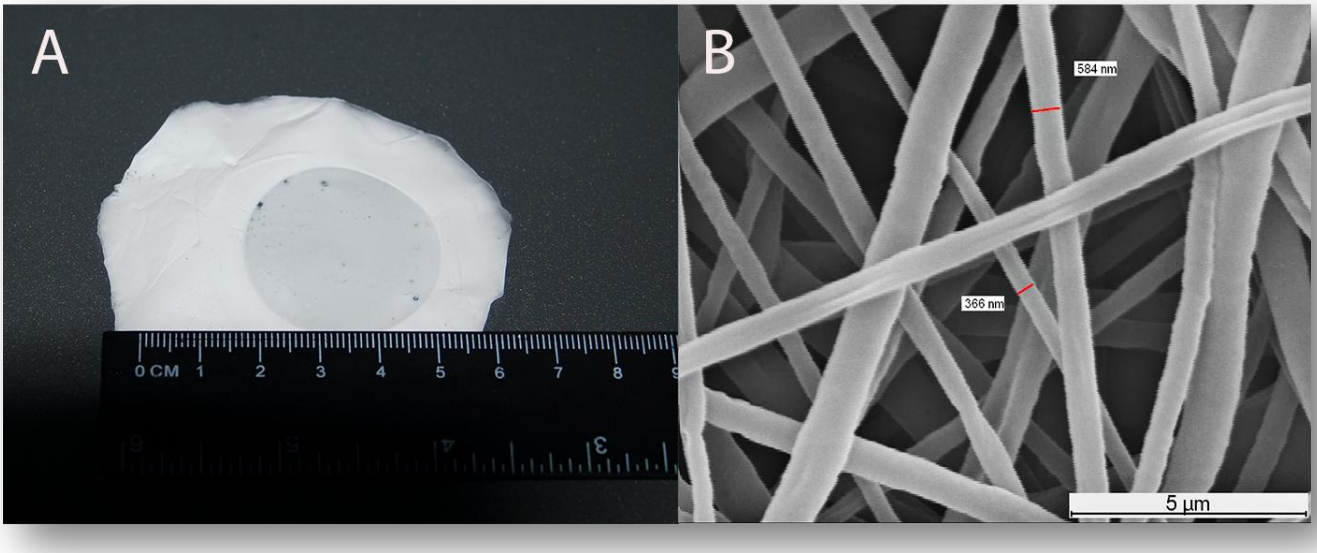

Figure 14- Images of an electrospun nanofiber membrane (ENM). A- Macroscopic view. B- SEM view.

Moreover, the size of the produced membranes where optimized in order to increase the density of nanofibers and to facilitate the permeation studies (Fig. 15-A). Once decreased the surface area of the nanofibers, it was expected that for the same parameters of production the accumulation of nanofibers was higher (Fig. 15-B). The nanofibers presented in this figure are randomly distributed with absence of beads.

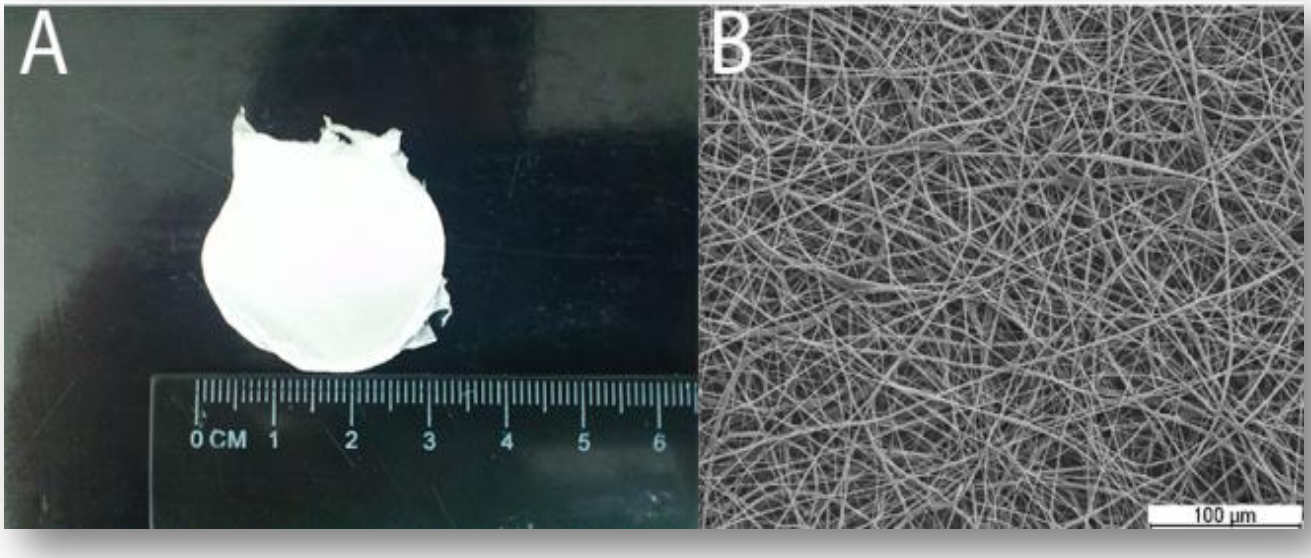

Figure 15 – Images of the Macroscopic view of ENM with optimized size (A) and by SEM (B).

The decrease of the membrane size made the mesh density higher. The PEO-SA and PVP electrospun nanofibers were compared in order to evaluate which of them had fibers with a low diameter. As it was possible to visualize by the measures in SEM images above, the PEO-SA nanofibers showed a smaller diameter when compared to the PVP nanofibers (Fig.16). Consequently, a new layer of nanofibers of PEO-SA was applied to the main support membrane (Fig.17). Then, the membrane was submitted to PEO-SA coating and crosslinked in calcium chloride for 48h, in order to maintain the new layer created under the PCL support. The new coating was made with the purpose of reducing the pore size of membranes for causing retention of the pretended bioactive biomolecules. However, the decreasing of pore size can only be expected if the density of this kind of fibers is increased. These membranes proof to be useful for phase separation area. The mesh of nanofibers had a similar area to that of commercial membranes [91]

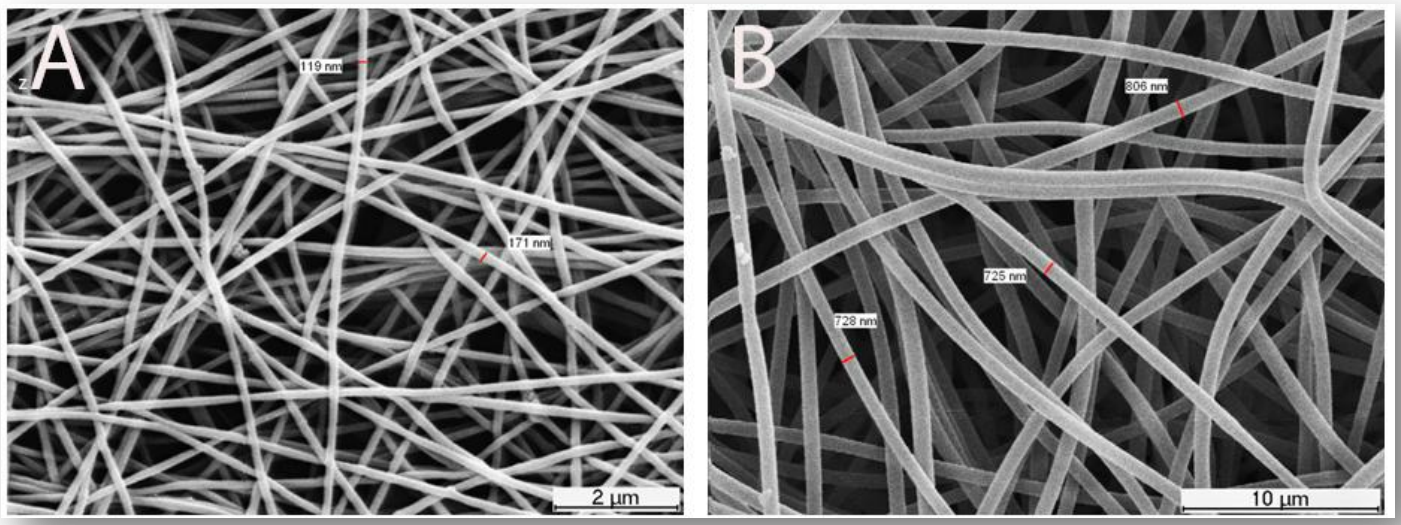

Figure 16 - SEM images of PEO-SA nanofibers (A) and PVP nanofibers (B)

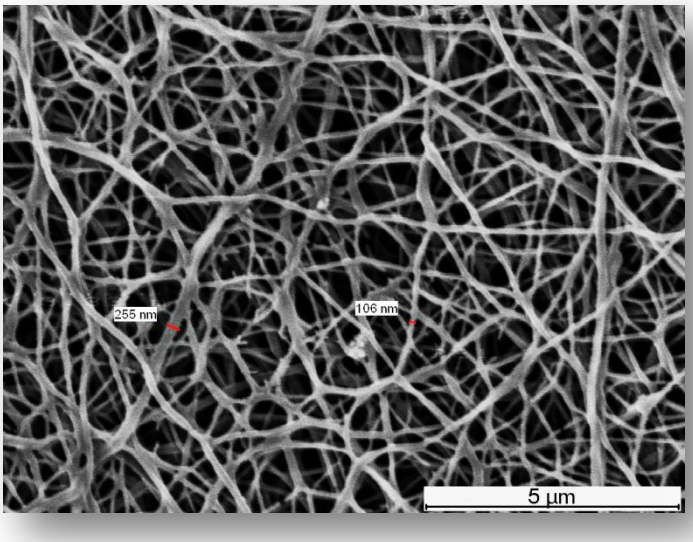

Figure 17 - PCL ENM coated with PEO-SA

Table 6- Parameters optimized for the production of electrospun nanofiber membranes

ENM	Deposition time (min)	Concentration (%)	Collector dimension (cm^2)	PEO-SA coating time (min)	Crosslinking time (hours)
PCL	40	10	129,15	20	12
PCL	25	10	4,1	15	12

3.3 Fourier transform infrared spectroscopy – analysis of the ENM surfaces

ATR-FTIR analysis was carried out for surface characterization of the PCL nanofiber membrane in the range of 400–4000 cm^{-1}. The characteristic peak centered at 1722 cm^{-1}, was observed for the PCL nanofiber membrane (Fig.18). The former one, caused by the hydroxyl stretching vibration, was relatively weak, and the latter one was derived from the C=O stretching of ester group [92]. Furthermore, in the C-H stretching region of FTIR spectrum, the higher intensity peak at 2944 cm^{-1} was assigned to the asymmetric and the lower intensity peak at 2867 cm^{-1} was assigned to the symmetric modes of CH_2 [93]. The other surface of the PCL membrane was also analyzed by ATR-FTIR. Sodium alginate is a polyelectrolyte that possesses high conductivity and can form solutions with a wide range of viscosity. After be blent with PEO, the interaction formed between PEO and sodium alginate reduces the repulsive force among polyanionic sodium alginate molecules, and thus allows successful electrospinning of sodium alginate/PEO blends, that was demonstrated by conductivity change and FTIR. In FTIR spectra (Fig. 19), as the proportion of PEO in blends increases from 0% to 50%, the asymmetrical band of carboxylate ion has shifted to lower frequencies from 1593 cm^{-1} to 1613 cm^{-1}, and the hydroxy band of sodium alginate has shifted from 3246 cm^{-1} to 3406 cm^{-1}, revealing interaction of sodium alginate and PEO through hydrogen bonding between the etheric oxygen of PEO and hydroxyl groups of sodium alginate [94].

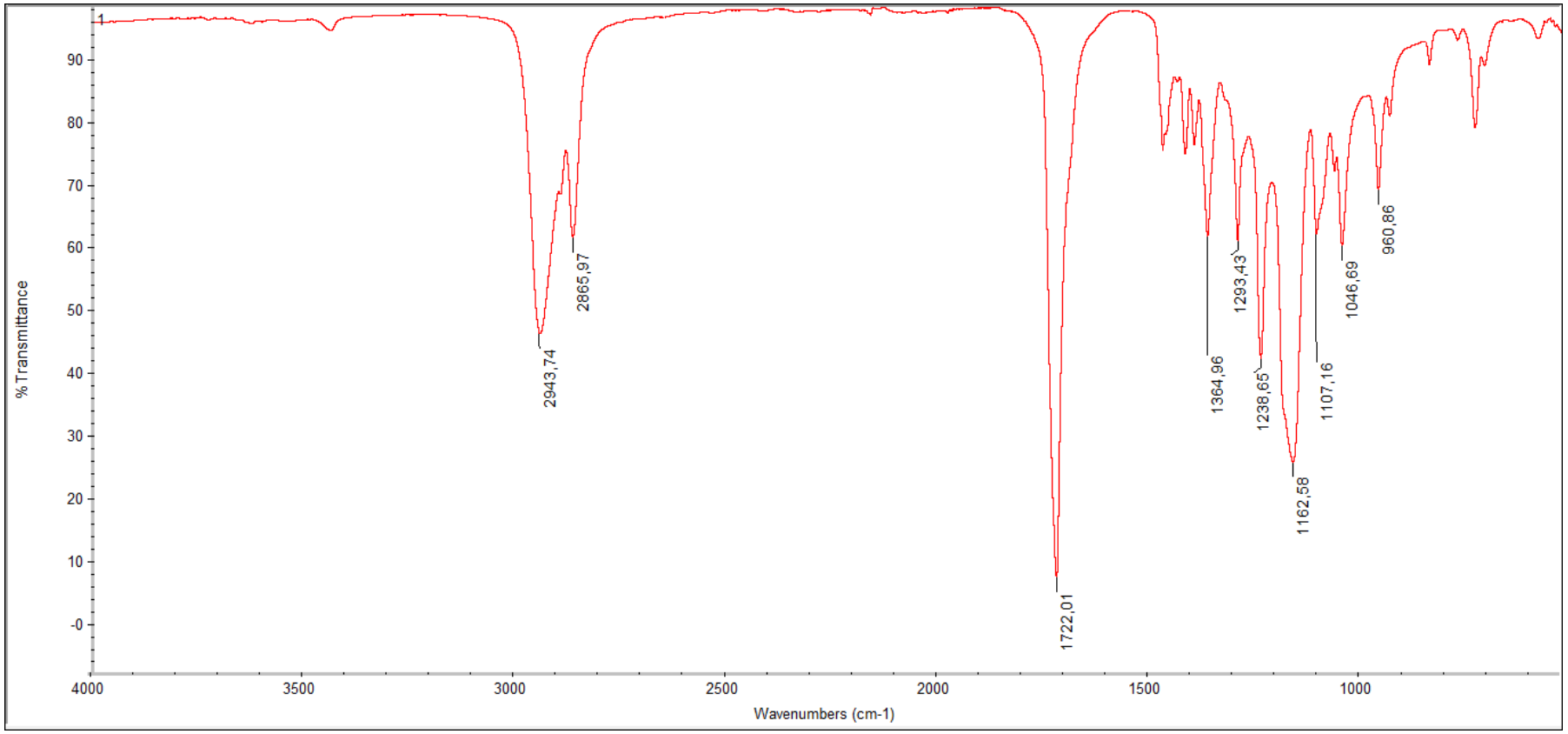

Figure 18- FTIR spectra of the produced PCL nanofiber membrane.

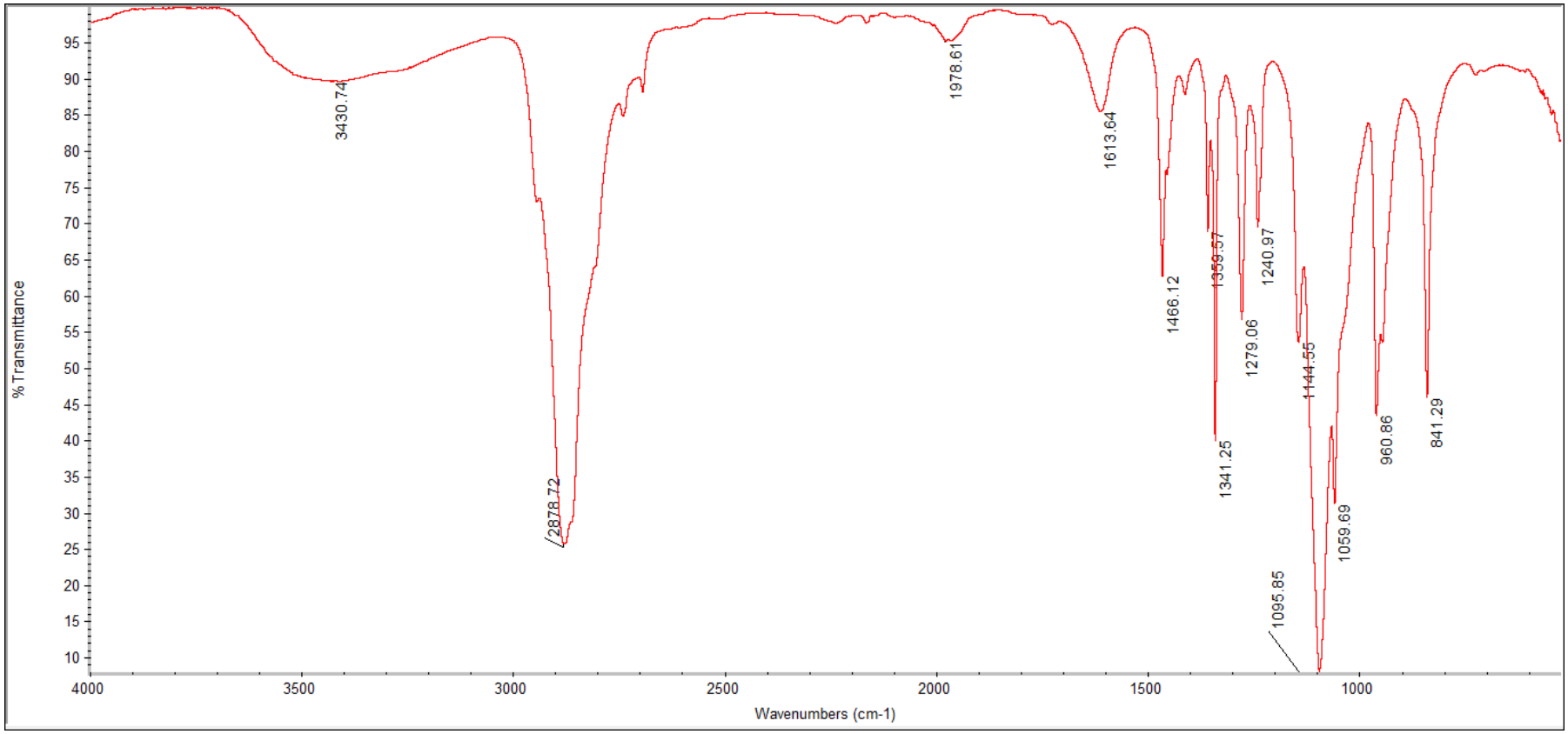

Figure 19- FTIR spectra of the produced PEO-SA coating nanofiber layer.

3.4 Evaluation of the cytotoxic profile of the different coatings on the scaffold

The cytocompatibility of the coated scaffolds was evaluated through *in vitro* studies. As described before, human osteoblast cells were seeded at the same density in the 96 well plates, with and without materials to assess its cytoxicity. In the first 24 h, cell adhesion and proliferation was observed in wells where they were in contact with the materials (Fig 20-A,B,C,D) and in the negative control (Fig.20-E). In the positive control, no cell adhesion or proliferation was observed. Dead cells with their typical spherical shape were visualized in figure 20-F. After 48 h, cells continue to proliferate in wells where they were in contact with the materials and in the negative control. In positive control no proliferation was noticed (Fig.20-L). The observation of cell growth in the presence of materials during 48 h demonstrated that cells in contact with the scaffold coated by PCL nanofibers presented the higher proliferation, which is similar to that observed in the negative control. On the other hand, cells in contact with the scaffold without coating had the lowest proliferation. The relative increase on cell proliferation for alginate scaffolds coated with PCL nanofibers, when compared to that observed for alginate scaffolds solely, indicates that coating the materials with PCL nanofibers can bring benefits in terms of biocompatibility due to an increasing of the surface area that allows a better cell adhesion. In the same way, the PEO-SA and PVP coating nanofibers also demonstrated an increase on cellular viability when compared to alginate scaffold solely. To further evaluate the cytotoxic profile of the materials, MTS assay was also performed. The MTS assay results (Fig.21) showed that cell viability was higher for the negative control, in which cells were seeded just with DMEM-F12. Cells seeded in the presence of PEO-SA, PVP and PCL nanofibers showed that cell viability was maintained over time, higher than positive control and near to negative control. The MTS assay showed a significant difference between positive control and the negative control and cells exposed to materials over 48 h of incubation (*$p<0.05$). Furthermore, all the coatings preformed with the different nanofibers improved the biological properties of the SA scaffold. Furthermore, to further characterize the biocompatibility of PCL nanofibers, SEM images of alginate microparticle scaffold coated with PCL nanofibers with Human osteoblast cells seeded on its surface were also acquired (Fig.22) In the figure 22 it is possible to observe cell spreading as well as the *filopodia* phenomenon, which shows membrane cellular prolongations on the surface of the material.

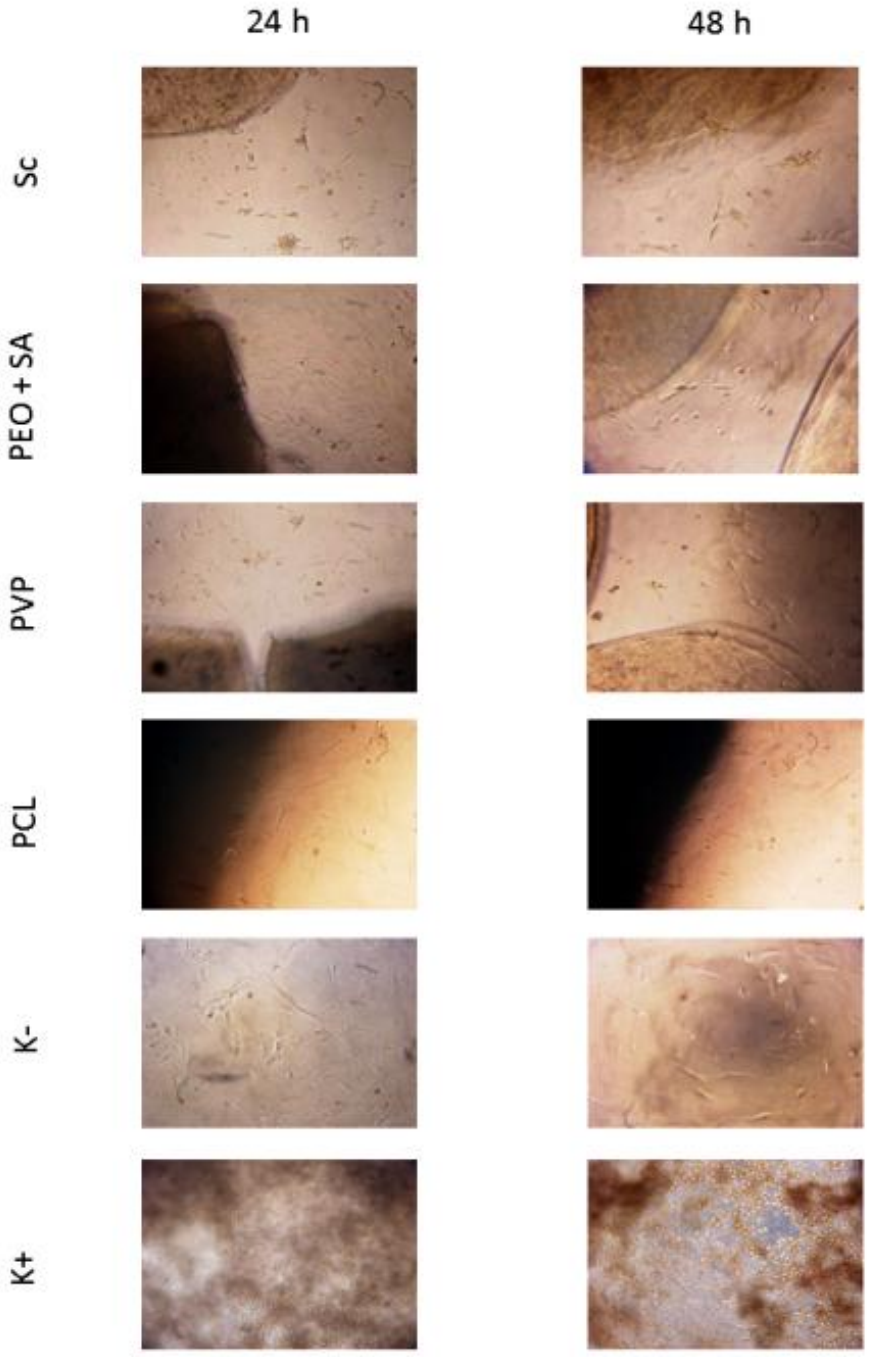

Figure 20- Optical microscopic photographs of human osteoblast cells after 24 and 48 h of being seeded: in the presence of scaffold without coating (Sc); in the presence of PEO combined with SA coated scaffolds; in the presence of PVP coated scaffolds; in the presence of PCL coated scaffolds; (K-) negative control; (K+) positive control. Original magnification x100.

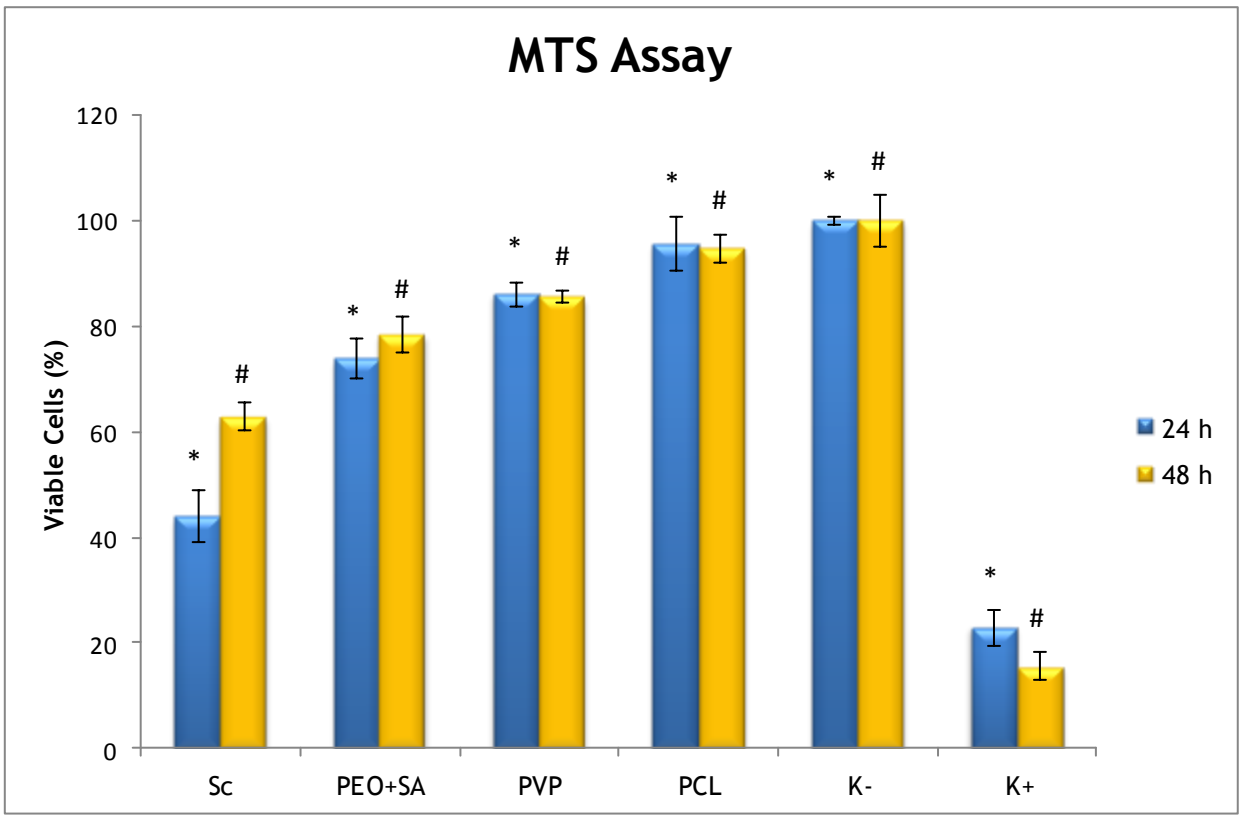

Figure 21 - Cellular activities measured by the MTS assay after 24 and 48 h of being seeded: the presence of scaffold without coating (Sc); in the presence of PEO combined with SA coated scaffolds; in the presence of PVP coated scaffolds; in the presence of PCL coated scaffolds; (K+) positive control; (K-) negative control. Each result is the mean standard error of the mean of at least three independent experiments. Statistical analysis was performed using one-way ANOVA with Dunnet's post hoc test (*$p<0.05$; # $p<0.05$).).

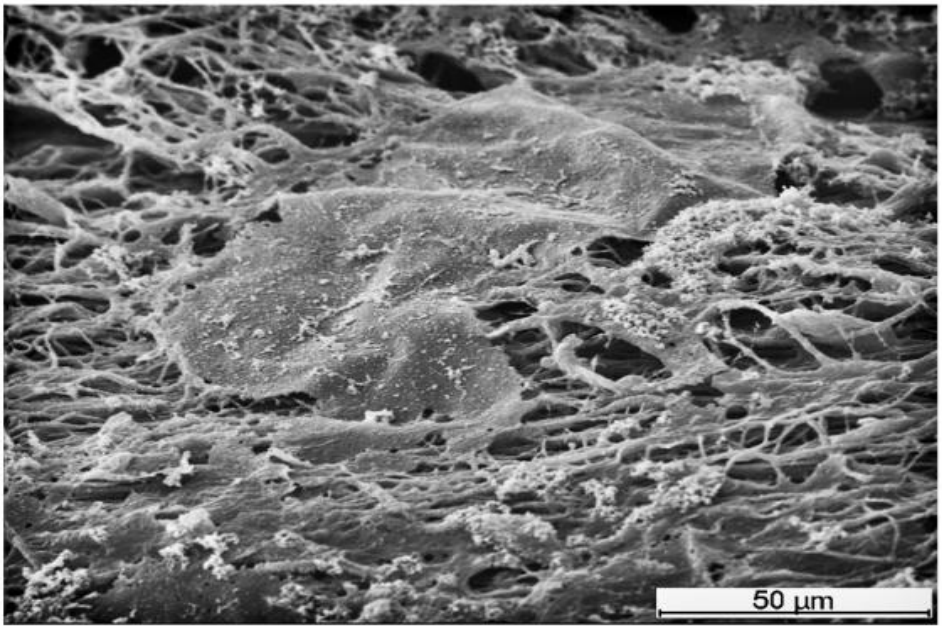

Figure 22- SEM image acquired after 24h of Human osteoblast cells have been placed in contact with the alginate microparticle scaffold coated with PCL nanofibers.

Chapter IV:
Conclusions and Future Perspectives

A lot of research has been done in the area of Tissue Engineering in order to find better solutions for the regeneration of biological tissues. In this study, it was developed a coating method for 3D scaffolds using electrospun polymeric nanofibers, in order to be applied for bone tissue regeneration. The polymeric nanofibers were successfully produced in our laboratory through the optimization of parameters such as voltage, flux and polymer concentration. Then, 3D scaffolds were coated with different nanofibers and ENMs were produced with various materials. Based on the results obtained, it was possible to verify that PCL nanofibers have a wide range of diameters. On the other hand PEO-SA nanofibers showed to be smallers than the others and the range of their dimension was lower when compared to the PCL nanofibers. The evaluation of cytotoxic profiles showed that the nanofibers used to perform the coating of SA scaffold enhanced its biocompatibility. However, the results showed that a higher cellular viability was obtained for the PCL nanofibers, which were the fibers where the size range was more divergent. With these kinds of electrospun polymeric nanofibers, the surface area was increased through the deposition of fibers for 10min. The produced ENMs with PCL were achieved through the increasing of deposition time of the polymer. Additionally, the pore size was reduced by the deposition of a new layer of PEO-SA nanofibers under the ENM of PCL that could be visualized by the density of nanofibers and also by its diameter. This coating on the ENM created a denser mesh and subsequently increased the permeability of the membrane, which is extremely useful for their use in the micro or ultrafiltration process of bioactive biomolecules or even on the filtration of plasmid DNA (pDNA). The results herein presented show that the polymeric nanofiber coatings and membranes have a huge potential to be applied on Tissue Engineering or in other areas such as Phase Separation. On a tissue engineering perspective, these nanofiber coatings can be produced based on the type of tissue to be regenerated and in the future they can also be used to incorporate growth factors as well as other bioactive biomolecules, to characterize the tissue regeneration. Moreover, the combination between different polymers has a great potential due to the combination of specific properties of each the polymers in an unique polymeric solution. The electrospun nanofiber membranes (ENMs) produced and studied for phase separation applications can be improved through the use of new polymers or even through the improvement of the production parameters, such as needle size and type, deposition time or collector type, number of layers, among others.

Chapter V:
References

1. Jang, J.H., O. Castano, and H.W. Kim, *Electrospun materials as potential platforms for bone tissue engineering*. Advanced drug delivery reviews, 2009. **61**(12): p. 1065-1083.
2. Michael H. Ross, W.P., *Histology: a text and atlas: with correlated cell and molecular biology* 6th ed2011. 996
3. Djouad, F., D. Guerit, M. Marie, K. Toupet, C. Jorgensen, and D. Noel, *Mesenchymal Stem Cells: New Insights into Bone Regenerative Applications*. Journal of Biomaterials and Tissue Engineering, 2012. **2**(1): p. 14-28.
4. Xu, W., X. Liao, B. Li, and T. Li. *Biomaterials and bone tissue engineering*. 2011. IEEE.
5. James, R., M. Deng, C.T. Laurencin, and S.G. Kumbar, *Nanocomposites and bone regeneration*. Frontiers of Materials Science, 2011: p. 1-16.
6. Murugan, R. and S. Ramakrishna, *Development of nanocomposites for bone grafting*. Composites Science and Technology, 2005. **65**(15-16): p. 2385-2406.
7. Ralston, S.H., *Bone structure and metabolism*. 2009. **37**(9): p. 469-474.
8. Shekaran, A. and A.J. García, *Extracellular matrix-mimetic adhesive biomaterials for bone repair*. Journal of Biomedical Materials Research Part A, 2011. **96**(1): p. 261-272.
9. Bab, I., B. Ashton, D. Gazit, G. Marx, M. Williamson, and M. Owen, *Kinetics and differentiation of marrow stromal cells in diffusion chambers in vivo*. Journal of cell science, 1986. **84**(1): p. 139.
10. Skerry, T.M., L.E. Lanyon, L. Bitensky, and J. Chayen, *Early strain-related changes in enzyme activity in osteocytes following bone loading in vivo*. Journal of Bone and Mineral Research, 1989. **4**(5): p. 783-788.
11. Li, Z., K. Kong, and W. Qi, *Osteoclast and its roles in calcium metabolism and bone development and remodeling*. Biochemical and biophysical research communications, 2006. **343**(2): p. 345-350.
12. Jee, W., *Integrated bone tissue physiology: anatomy and physiology*. Bone mechanics handbook, 2001. **2**: p. 1.1-1.68.
13. Blair, H.C., S.L. Teitelbaum, R. Ghiselli, and S. Gluck, *Osteoclastic bone resorption by a polarized vacuolar proton pump*. Science, 1989. **245**(4920): p. 855.
14. Gelse, K., E. Pöschl, and T. Aigner, *Collagens--structure, function, and biosynthesis*. Advanced drug delivery reviews, 2003. **55**(12): p. 1531-1546.

15. Robey, P.G. and A.L. Boskey, . *The Composition of Bone*. Primer on the Metabolic Bone Diseases and Disorders of Mineral Metabolism, 2008: p. 32-38.
16. Aubin, J.E. and J.T. Triffitt, *Mesenchymal stem cells and osteoblast differentiation*. Principles of bone biology, 2002. **1**: p. 59-81.
17. Gaalen, S.v., M. Kruyt, G. Meijer, A. Mistry, A. Mikos, J.v.d. Beucken, J. Jansen, K.d. Groot, R. Cancedda, C. Olivo, M. Yaszemski, and W. Dhert, *Chapter 19 - Tissue engineering of bone*, in *Tissue Engineering*, B. Clemens van, et al., Editors. 2008, Academic Press: Burlington. p. 559-610.
18. Karsenty, G., H.M. Kronenberg, and C. Settembre, *Genetic control of bone formation*. Annual Review of Cell and Developmental, 2009. **25**: p. 629-648.
19. Schett, G. and J.P. David, *The multiple faces of autoimmune-mediated bone loss*. Nature Reviews Endocrinology, 2010. **6**(12): p. 698-706.
20. Schett, G., S. Kiechl, S. Weger, A. Pederiva, A. Mayr, M. Petrangeli, F. Oberhollenzer, R. Lorenzini, K. Redlich, and R. Axmann, *High-sensitivity C-reactive protein and risk of nontraumatic fractures in the Bruneck study*. Archives of internal medicine, 2006. **166**(22): p. 2495.
21. Feng, X. and J.M. McDonald, *Disorders of bone remodeling*. Annual Review of Pathology: Mechanisms of Disease, 2011. **6**: p. 121-145.
22. Cheung, M. and F. Glorieux, *Osteogenesis Imperfecta: Update on presentation and management*. Reviews in Endocrine & Metabolic Disorders, 2008. **9**(2): p. 153-160.
23. Ngiam, M., L. Nguyen, S. Liao, C. Chan, and S. Ramakrishna, *Biomimetic Nanostructured Materials—Potential Regulators for Osteogenesis?* Annals of the Academy of Medicine, Singapore, 2011. **40**(5): p. 213.
24. Holzwarth, J.M. and P.X. Ma, *Biomimetic nanofibrous scaffolds for bone tissue engineering*. Biomaterials, 2011.
25. Lee, K.J.H., J.G. Roper, and J.C. Wang, *Demineralized bone matrix and spinal arthrodesis*. The Spine Journal, 2005. **5**(6): p. S217-S223.
26. Both, S.K., A.J.C. Muijsenberg, C.A. Blitterswijk, J. Boer, and J.D. Bruijn, *A rapid and efficient method for expansion of human mesenchymal stem cells*. Tissue engineering, 2007. **13**(1): p. 3-10.
27. Tian, X., B. Heng, Z. Ge, K. Lu, A. Rufaihah, V. Fan, J. Yeo, and T. Cao, *Comparison of osteogenesis of human embryonic stem cells within 2D and 3D culture systems*. Scandinavian journal of clinical and laboratory investigation, 2008. **68**(1): p. 58.

28. Di Martino, A., L. Liverani, A. Rainer, G. Salvatore, M. Trombetta, and V. Denaro, *Electrospun scaffolds for bone tissue engineering*. Musculoskeletal surgery, 2011: p. 1-12.
29. Liu, X. and P.X. Ma, *Polymeric Scaffolds for Bone Tissue Engineering: on Musculoskeletal Bioengineering. Guest Editor: Kyriacos A. Athanasiou*. Annals of Biomedical Engineering, 2004. **32**(3): p. 477-486.
30. Meyer, U. and H.P. Wiesmann, *Bone and cartilage engineering*2006: Springer Verlag.
31. Matsuoka, H., H. Akiyama, Y. Okada, H. Ito, C. Shigeno, J. Konishi, T. Kokubo, and T. Nakamura, *In vitro analysis of the stimulation of bone formation by highly bioactive apatite-and wollastonite-containing glass-ceramic: Released calcium ions promote osteogenic differentiation in osteoblastic ROS17/2.8 cells*. Journal of biomedical materials research, 1999. **47**(2): p. 176-188.
32. Beachley, V. and X. Wen, *Polymer nanofibrous structures: Fabrication, biofunctionalization, and cell interactions*. Progress in Polymer Science, 2010. **35**(7): p. 868-892.
33. Leong, M.F., K.S. Chian, P.S. Mhaisalkar, W.F. Ong, and B.D. Ratner, *Effect of electrospun poly (D, L-lactide) fibrous scaffold with nanoporous surface on attachment of porcine esophageal epithelial cells and protein adsorption*. Journal of Biomedical Materials Research Part A, 2009. **89**(4): p. 1040-1048.
34. Baker, B.M., A.O. Gee, R.B. Metter, A.S. Nathan, R.A. Marklein, J.A. Burdick, and R.L. Mauck, *The potential to improve cell infiltration in composite fiber-aligned electrospun scaffolds by the selective removal of sacrificial fibers*. Biomaterials, 2008. **29**(15): p. 2348-2358.
35. Li, X., H. Gao, M. Uo, Y. Sato, T. Akasaka, Q. Feng, F. Cui, X. Liu, and F. Watari, *Effect of carbon nanotubes on cellular functions in vitro*. Journal of Biomedical Materials Research Part A, 2009. **91**(1): p. 132-139.
36. Fu, X., H. Matsuyama, M. Teramoto, and H. Nagai, *Preparation of hydrophilic poly(vinyl butyral) hollow fiber membrane via thermally induced phase separation*. Separation and Purification Technology, 2005. **45**(3): p. 200-207.
37. Lu, H., L. Zhang, W. Xing, H. Wang, and N. Xu, *Preparation of TiO2 hollow fibers using poly(vinylidene fluoride) hollow fiber microfiltration membrane as a template*. Materials Chemistry and Physics, 2005. **94**(2–3): p. 322-327.

38. Williamson, M.R. and A.G.A. Coombes, *Gravity spinning of polycaprolactone fibres for applications in tissue engineering*. Biomaterials, 2004. **25**(3): p. 459-465.
39. Hartgerink, J.D., E. Beniash, and S.I. Stupp, *Peptide-amphiphile nanofibers: a versatile scaffold for the preparation of self-assembling materials*. Proceedings of the National Academy of Sciences, 2002. **99**(8): p. 5133.
40. Kulkarni, A., V. Bambole, and P. Mahanwar, *Electrospinning of Polymers, Their Modeling and Applications*. Polymer-Plastics Technology and Engineering, 2010. **49**(5): p. 427-441.
41. Ashammakhi, N., A. Ndreu, Y. Yang, H. Ylikauppila, and L. Nikkola, *Nanofiber-based scaffolds for tissue engineering*. European Journal of Plastic Surgery, 2012. **35**(2): p. 135-149.
42. Zhao, Z., J. Zheng, M. Wang, H. Zhang, and C.C. Han, *High performance ultrafiltration membrane based on modified chitosan coating and electrospun nanofibrous PVDF scaffolds*. Journal of membrane science, 2012. **394-395**: p. 209-217.
43. Dahlin, R.L., F.K. Kasper, and A.G. Mikos, *Polymeric Nanofibers in Tissue Engineering*. Tissue Engineering Part B: Reviews, 2011. **17**(5): p. 349-364.
44. Bhardwaj, N. and S.C. Kundu, *Electrospinning: A fascinating fiber fabrication technique*. Biotechnology Advances, 2010. **28**(3): p. 325-347.
45. Xu, L., *A mathematical model for electrospinning process under coupled field forces*. Chaos, Solitons & Fractals, 2009. **42**(3): p. 1463-1465.
46. Secasanu, V.P., C.K. Giardina, and Y. Wang, *A novel electrospinning target to improve the yield of uniaxially aligned fibers*. Biotechnology progress, 2009. **25**(4): p. 1169-1175.
47. Salem, D.R., *Structure formation in polymeric fibers*2001: Hanser Gardner Pubns.
48. Deitzel, J., J. Kleinmeyer, J. Hirvonen, and N. Beck Tan, *Controlled deposition of electrospun poly (ethylene oxide) fibers*. Polymer, 2001. **42**(19): p. 8163-8170.
49. Liao, S., C.K. Chan, and S. Ramakrishna, *Electrospun nanofibers: Work for medicine?* Frontiers of Materials Science in China, 2010. **4**(1): p. 29-33.
50. Huang, Z.M., Y.Z. Zhang, M. Kotaki, and S. Ramakrishna, *A review on polymer nanofibers by electrospinning and their applications in nanocomposites*. Composites Science and Technology, 2003. **63**(15): p. 2223-2253.

51. Lim, S.H. and H.-Q. Mao, *Electrospun scaffolds for stem cell engineering*. Advanced Drug Delivery Reviews, 2009. **61**(12): p. 1084-1096.
52. Flemming, R., C. Murphy, G. Abrams, S. Goodman, and P. Nealey, *Effects of synthetic micro-and nano-structured surfaces on cell behavior*. Biomaterials, 1999. **20**(6): p. 573-588.
53. Green, A.M., J.A. Jansen, J. Van der Waerden, and A.F. Von Recum, *Fibroblast response to microtextured silicone surfaces: Texture orientation into or out of the surface*. Journal of biomedical materials research, 1994. **28**(5): p. 647-653.
54. Sharma, B. and J.H. Elisseeff, *Engineering structurally organized cartilage and bone tissues*. Annals of Biomedical Engineering, 2004. **32**(1): p. 148-159.
55. Sill, T.J. and H.A. Von Recum, *Electrospinning: applications in drug delivery and tissue engineering*. Biomaterials, 2008. **29**(13): p. 1989-2006.
56. Ramakrishna, S., *An introduction to electrospinning and nanofibers*2005: World Scientific Pub Co Inc.
57. Deitzel, J., J. Kleinmeyer, D. Harris, and N. Beck Tan, *The effect of processing variables on the morphology of electrospun nanofibers and textiles*. Polymer, 2001. **42**(1): p. 261-272.
58. Zuo, W., M. Zhu, W. Yang, H. Yu, Y. Chen, and Y. Zhang, *Experimental study on relationship between jet instability and formation of beaded fibers during electrospinning*. Polymer Engineering & Science, 2005. **45**(5): p. 704-709.
59. Pattamaprom, C., W. Hongrojjanawiwat, P. Koombhongse, P. Supaphol, T. Jarusuwannapoo, and R. Rangkupan, *The influence of solvent properties and functionality on the electrospinnability of polystyrene nanofibers*. Macromolecular Materials and Engineering, 2006. **291**(7): p. 840-847.
60. Uyar, T. and F. Besenbacher, *Electrospinning of uniform polystyrene fibers: The effect of solvent conductivity*. Polymer, 2008. **49**(24): p. 5336-5343.
61. Kwak, G., G.H. Lee, S. Shim, and K.B. Yoon, *Fabrication of Light-Guiding Core/Sheath Fibers by Coaxial Electrospinning*. Macromolecular Rapid Communications, 2008. **29**(10): p. 815-820.
62. Bhattarai, N., Z. Li, D. Edmondson, and M. Zhang, *Alginate-based nanofibrous scaffolds: Structural, mechanical, and biological properties*. Advanced Materials, 2006. **18**(11): p. 1463-1467.
63. Tuzlakoglu, K., N. Bolgen, A. Salgado, M. Gomes, E. Piskin, and R. Reis, *Nano-and micro-fiber combined scaffolds: a new architecture for bone tissue*

engineering. Journal of Materials Science: Materials in Medicine, 2005. **16**(12): p. 1099-1104.

64. Pattison, M.A., S. Wurster, T.J. Webster, and K.M. Haberstroh, *Three-dimensional, nano-structured PLGA scaffolds for bladder tissue replacement applications*. Biomaterials, 2005. **26**(15): p. 2491-2500.
65. Nemir, S. and J.L. West, *Synthetic materials in the study of cell response to substrate rigidity*. Annals of Biomedical Engineering, 2010. **38**(1): p. 2-20.
66. Tuzlakoglu, K. and R.L. Reis, *Biodegradable polymeric fiber structures in tissue engineering*. Tissue Engineering Part B: Reviews, 2008. **15**(1): p. 17-27.
67. Nie, H., A. He, J. Zheng, S. Xu, J. Li, and C.C. Han, *Effects of chain conformation and entanglement on the electrospinning of pure alginate*. Biomacromolecules, 2008. **9**(5): p. 1362-1365.
68. Francis Suh, J.K. and H.W.T. Matthew, *Application of chitosan-based polysaccharide biomaterials in cartilage tissue engineering: a review*. Biomaterials, 2000. **21**(24): p. 2589-2598.
69. Hsu, S.-h., S.W. Whu, S.-C. Hsieh, C.-L. Tsai, D.C. Chen, and T.-S. Tan, *Evaluation of Chitosan-alginate-hyaluronate Complexes Modified by an RGD-containing Protein as Tissue-engineering Scaffolds for Cartilage Regeneration*. Artificial Organs, 2004. **28**(8): p. 693-703.
70. Chen, J., B. Chu, and B.S. Hsiao, *Mineralization of hydroxyapatite in electrospun nanofibrous poly (L-lactic acid) scaffolds*. Journal of Biomedical Materials Research Part A, 2006. **79**(2): p. 307-317.
71. Ito, Y., H. Hasuda, M. Kamitakahara, C. Ohtsuki, M. Tanihara, I.K. Kang, and O.H. Kwon, *A composite of hydroxyapatite with electrospun biodegradable nanofibers as a tissue engineering material*. Journal of bioscience and bioengineering, 2005. **100**(1): p. 43-49.
72. Kim, H.N., D.H. Kang, M.S. Kim, A. Jiao, D.H. Kim, and K.Y. Suh, *Patterning Methods for Polymers in Cell and Tissue Engineering*. Annals of Biomedical Engineering, 2012: p. 1-17.
73. Li, C., C. Vepari, H.-J. Jin, H.J. Kim, and D.L. Kaplan, *Electrospun silk-BMP-2 scaffolds for bone tissue engineering*. Biomaterials, 2006. **27**(16): p. 3115-3124.
74. Tuzlakoglu, K., N. Bolgen, A. Salgado, M. Gomes, E. Piskin, and R. Reis, *Nano- and micro-fiber combined scaffolds: A new architecture for bone tissue*

engineering. Journal of Materials Science: Materials in Medicine, 2005. **16**(12): p. 1099-1104.

75. Yoshimoto, H., Y.M. Shin, H. Terai, and J.P. Vacanti, *A biodegradable nanofiber scaffold by electrospinning and its potential for bone tissue engineering*. Biomaterials, 2003. **24**(12): p. 2077-2082.
76. Fujihara, K., M. Kotaki, and S. Ramakrishna, *Guided bone regeneration membrane made of polycaprolactone/calcium carbonate composite nanofibers*. Biomaterials, 2005. **26**(19): p. 4139-4147.
77. Badami, A.S., M.R. Kreke, M.S. Thompson, J.S. Riffle, and A.S. Goldstein, *Effect of fiber diameter on spreading, proliferation, and differentiation of osteoblastic cells on electrospun poly(lactic acid) substrates*. Biomaterials, 2006. **27**(4): p. 596-606.
78. Ionescu, L.C., G.C. Lee, B.J. Sennett, J.A. Burdick, and R.L. Mauck, *An anisotropic nanofiber/microsphere composite with controlled release of biomolecules for fibrous tissue engineering*. Biomaterials, 2010. **31**(14): p. 4113-4120.
79. Zargarian, S.S. and V. Haddadi-Asl, *A nanofibrous composite scaffold of PCL/hydroxyapatite-chitosan/PVA prepared by electrospinning*. Iran Polym J, 2010. **19**: p. 457-468.
80. Chuangchote, S., T. Sagawa, and S. Yoshikawa, *Electrospinning of poly (vinyl pyrrolidone): Effects of solvents on electrospinnability for the fabrication of poly (p-phenylene vinylene) and TiO2 nanofibers*. Journal of Applied Polymer Science, 2009. **114**(5): p. 2777-2791.
81. Ma, G., D. Fang, Y. Liu, X. Zhu, and J. Nie, *Electrospun sodium alginate/poly (ethylene oxide) core-shell nanofibers scaffolds potential for tissue engineering applications*. Carbohydrate Polymers, 2011.
82. Hiep, N.T. and B.T. Lee, *Electro-spinning of PLGA/PCL blends for tissue engineering and their biocompatibility*. Journal of Materials Science: Materials in Medicine, 2010. **21**(6): p. 1969-1978.
83. Gaspar, V., F. Sousa, J. Queiroz, and I. Correia, *Formulation of chitosan-TPP-pDNA nanocapsules for gene therapy applications*. Nanotechnology, 2011. **22**: p. 015101.
84. Bacsik, Z., J. Mink, and G. Keresztury, *FTIR Spectroscopy of the Atmosphere. I. Principles and Methods*. Applied Spectroscopy Reviews, 2004. **39**(3): p. 295-363.

85. Lopérgolo, L.C., A.B. Lugão, and L.H. Catalani, *Direct UV photocrosslinking of poly (< i> N-vinyl-2-pyrrolidone)(PVP) to produce hydrogels*. Polymer, 2003. **44**(20): p. 6217-6222.
86. Maia, J., M.P. Ribeiro, C. Ventura, R.A. Carvalho, I.J. Correia, and M.H. Gil, *Ocular injectable formulation assessment for oxidized dextran-based hydrogels*. Acta Biomaterialia, 2009. **5**(6): p. 1948-1955.
87. Ribeiro, M.P., A. Espiga, D. Silva, P. Baptista, J. Henriques, C. Ferreira, J.C. Silva, J.P. Borges, E. Pires, P. Chaves, and I.J. Correia, *Development of a new chitosan hydrogel for wound dressing*. Wound Repair and Regeneration, 2009. **17**(6): p. 817-824.
88. Palmeira-de-Oliveira, A., M.P. Ribeiro, R. Palmeira-de-Oliveira, C. Gaspar, S. Costa-de-Oliveira, I.J. Correia, C. Pina Vaz, J. Martinez-de-Oliveira, J.A. Queiroz, and A.G. Rodrigues, *Anti-Candida Activity of a Chitosan Hydrogel: Mechanism of Action and Cytotoxicity Profile*. Gynecologic and Obstetric Investigation, 2010. **70**(4): p. 322-327.
89. Reneker, D., W. Kataphinan, A. Theron, E. Zussman, and A. Yarin, *Nanofiber garlands of polycaprolactone by electrospinning*. Polymer, 2002. **43**(25): p. 6785-6794.
90. Armentano, I., M. Dottori, E. Fortunati, S. Mattioli, and J. Kenny, *Biodegradable polymer matrix nanocomposites for tissue engineering: A review*. Polymer Degradation and Stability, 2010. **95**(11): p. 2126-2146.
91. Yoon, K., K. Kim, X. Wang, D. Fang, B.S. Hsiao, and B. Chu, *High flux ultrafiltration membranes based on electrospun nanofibrous PAN scaffolds and chitosan coating*. Polymer, 2006. **47**(7): p. 2434-2441.
92. Cho, H.H., D.-W. Han, K. Matsumura, S. Tsutsumi, and S.-H. Hyon, *The behavior of vascular smooth muscle cells and platelets onto epigallocatechin gallate-releasing poly(l-lactide-co-ε-caprolactone) as stent-coating materials*. Biomaterials, 2008. **29**(7): p. 884-893.
93. Kim, Y.J., M.R. Park, M.S. Kim, and O.H. Kwon, *Polyphenol-loaded polycaprolactone nanofibers for effective growth inhibition of human cancer cells*. Materials Chemistry and Physics, 2012.
94. Lu, J.W., Y.L. Zhu, Z.X. Guo, P. Hu, and J. Yu, *Electrospinning of sodium alginate with poly (ethylene oxide)*. Polymer, 2006. **47**(23): p. 8026-8031.